Summer 8-22-2019

A 2000 Year Detailed Climate Reconstruction Using a South Pole Ice Core

Elena Korotkikh
University of Maine, elena.korotkikh@maine.edu

Recommended Citation

Korotkikh, Elena, "A 2000 Year Detailed Climate Reconstruction Using a South Pole Ice Core" (2019). *Electronic Theses and Dissertations*. 3104.
https://digitalcommons.library.umaine.edu/etd/3104

A 2000 YEAR DETAILED CLIMATE RECONSTRUCTION USING A SOUTH POLE ICE CORE

By

Elena Korotkikh

B.Sc. Novosibirsk State University, 2004

M.S. University of Maine, 2009

A DISSERTATION

Submitted in Partial Fulfillment of the

Requirements for the Degree of

Doctor of Philosophy

(in Earth and Climate Studies)

The Graduate School

The University of Maine

August 2019

Advisory Committee:

Paul A. Mayewski, Professor, Climate Change Institute and School of Earth and Climate Sciences, Director of Climate Change Institute, Advisor

Andrei V. Kurbatov, Associate Professor, Climate Change Institute and School of Earth and Climate Sciences

Kirk A. Maasch, Professor, Climate Change Institute and School of Earth and Climate Sciences

Jefferson C. Simões, Professor, Universidade Federal do Rio Grande do Sul

Daniel A. Dixon, Research Assistant Professor, Climate Change Institute, Director of Sustainability

A 2000 YEAR DETAILED CLIMATE RECONSTRUCTION USING A SOUTH POLE ICE CORE

By Elena Korotkikh

Thesis Advisor: Dr. Paul A. Mayewski

An Abstract of the Dissertation Presented
in Partial Fulfillment of the Requirements for the
Degree of Doctor of Philosophy
(in Earth and Climate Studies)
August 2019

The research presented in this dissertation utilizes high-resolution records of major and trace elements, major ions, and stable water isotopes covering the last ~2000 years from the SPRESSO South Pole ice core to reconstruct past climate variability and evaluate anthropogenic impacts. The dissertation is in three parts. The first section demonstrates major reorganization of atmospheric circulation during the period 1400-1700 CE, and shows that this atmospheric reorganization occurred in two steps: ~1400-1425 CE and ~1650-1700 CE. Major declines in dust and SO_4^{2-} concentrations are observed ~1400 CE suggesting poleward contraction and intensification of westerly air flow. The changes in stable water isotopes, deuterium excess, NO_3^- concentration and accumulation rate characterize a second shift in atmospheric reorganization between 1650-1700 CE. The period since ~1650 CE is characterized by increased marine air mass incursions to South Pole, reduction of the katabatic winds, a poleward shift in the moisture source, and a sea ice decrease in the Weddell Sea.

The second part of the dissertation presents a high-resolution (~9 samples/year), continuous record of natural and anthropogenic source arsenic (As) deposition over the last

~2000 years. We show that volcanic and terrestrial biogenic emissions are a major natural source for As. We suggest that early human smelting activities could have contributed to the As deposition as early as 225 CE. The most significant anthropogenic source As enrichment in the record, starting in 1975 CE, is associated with increased copper production in Chile and at least partially to coal combustion from throughout the Southern Hemisphere.

The third part of the dissertation describes a record of barium deposition at the South Pole. Significant enrichment observed since 1980 CE is attributed to local pollution from activities at Amundsen-Scott South Pole Station.

ACKNOWLEDGEMENTS

I am very grateful to my advisor, Professor Paul Mayewski, for his supervision, many discussions, and constant help during my PhD. I am grateful for opportunities to visit many beautiful places doing field work and attending conferences.

I would like to thank my advisory committee members, Dr. Andrei Kurbatov, Dr. Dan Dixon, Dr. Kirk Maasch and Dr. Jefferson Simões, for the endless assistance and support throughout this project.

A special thanks to Sharon Sneed, Mike Handley, Cap Introne and Jay Holweger for all their help and hard work analyzing numerous amounts of samples. I thank Bjorn Grigholm for doing density measurements, and Jay Holweger and Justin Lambert for helping with core processing.

I thank my former fellow students Nicky Spaulding, Mario Potocki, Bjorn Grigholm, Jeff Auger, Charles Rodda, Mark Royer and Heather Clifford, for their friendship and support.

My sincere thanks to Betty Lee, Rebecca Addessi, Dianne Perro, Linda Cappuccio, Sarah Joughin, Mireille Le Gal, Debbi Clements and Katie Rossignol for all their help in the office.

Lastly, I would like to thank my family for their support and encouragement through all these years. Without you I would never have been able to accomplish it.

This research was supported by US National Science Foundation Office of Polar Programs grants PRL-1042883, 0439589, 0636506, 0829227, 1203640. I greatly acknowledge the support of the US Antarctic Program, the 109th New York Air National Guard, Ice Coring and Drilling Services, Raytheon Polar Services Company, the National Ice Core Laboratory, Kenn Borek Air Ltd., and all of our US ITASE field colleagues.

TABLE OF CONTENTS

LIST OF TABLES

LIST OF FIGURES

CHAPTER 1

INTRODUCTION

Ice core records are a robust tool for investigating past climate variability. Climate reconstructions based on glaciochemical records are useful for predicting future climate changes. This research presents high-resolution records of major and trace elements, major ions and stable water isotopes for the past ~2000 years using an ice core from South Pole. These glaciochemical records offer a detailed reconstruction of past climate variability, including changes in atmospheric chemistry, sea ice extent, temperature, precipitation, and atmospheric circulation. South Pole Ba and As records show evidence of anthropogenic pollution in Antarctica.

The body of this dissertation consists of five chapters. Chapter 1 is an introduction. Chapter 2 is a Methodology, it describes ice core collection and processing, sample analysis, and age model development. Chapters 3, 4 and 5 were written as individual papers for publication in peer-reviewed journals as described below.

Chapter 3 "Reorganization of atmospheric circulation between 1400-1700 CE as recorded in a South Pole ice core" focuses on changes in dust, SO_4^{2-}, NO_3^-, stable water isotopes and accumulation records covering the last 2000 years. Significant changes in chemical concentrations, accumulation rate, stable water isotopes, and deuterium excess records are demonstrated during the period ~1400-1700 CE indicating reorganization of atmospheric circulation.

Chapter 4 "A 2000-year record of arsenic variability from a South Pole ice core" presents a high-resolution (~9 samples/year), continuous record of arsenic (As) deposition at the South Pole and investigates natural and anthropogenic contributions. Our results show that volcanic emissions are a significant source of As for the South Pole, and that human activities might have contributed to As deposition as early as 225 CE. The most significant anthropogenic source As enrichment in the record, starting in 1975 CE, is linked to increased copper production in Chile and, at least partially, to coal combustion from throughout the Southern Hemisphere.

Chapter 5 “Recent increase in barium concentrations as recorded in a South Pole ice core” was published in 2014 in the Atmospheric Environment [*Korotkikh et al.*, 2014]. This chapter presents high-resolution (~9.4 samples/year) records of Ba concentrations for the period from 1541 to 1999 CE, and examines a significant increase in Ba concentration (by a factor of ~23) since 1980 CE. Comparison with other Antarctic Ba records suggests that the increase in Ba concentration at South Pole since 1980 CE is caused by local pollution from the Amundsen-Scott South Pole Station.

Chapter 6 “Conclusions” summarizes the major findings of this research.

CHAPTER 2

METHODOLOGY

2.1 Ice core collection and chemical analysis

The South Pole SPRESSO (South Pole Remote Earth Science and Seismological Observatory) ice core was drilled by ICDS (Ice Coring and Drilling Services) during the 2002-2003 Antarctic field season at 89.93°S, 144.39°W at an elevation of 2808 m a.s.l. and to a depth of 291.26 meters. The core was subsequently processed by the United States International Trans Antarctic Scientific Expedition team that assigned it the following core ID: US ITASE-02-6. No drilling fluid was used in the recovery of the core thus avoiding a major potential source of contamination.

The section from 0.8 to 200 meters of the South Pole ice core were melted using the Climate Change Institute continuous melting system [*Osterberg et al.*, 2006] at an average sample resolution of ~1 cm. Before melting, the ends of each section of ice were scraped inside a HEPA clean hood using a clean ceramic knife in an effort to prevent contamination. Melted co-registered samples were collected from the inner and outer parts of the core. To avoid contamination, only the inner portion of each sample was used for ICP-SFMS (Inductively Coupled Plasma Sector Field Mass Spectrometry) and IC (Ion Chromatography) analysis. Samples from the outer part of the core were collected for stable water isotopes analysis. ICP-SFMS samples were acidified to 1% with double-distilled HNO_3 and allowed to react with the acid for at least 2 months before analysis.

All samples were analyzed for their major anion (Cl^-, NO_3^-, SO_4^-) content using a Dionex DX-500 ion chromatograph paired to a Gilson Liquid Handler autosampler. Every sample from sections 0.88-59.4 m and 148.9-161 m depth (sample resolution 4-27 samples/year), and every tenth sample from the rest of the core (sample resolution 1-2 samples/year) were analyzed for major and trace elements (Na, Mg, Ca, Sr, Cd, Cs, Ba, La, Ce, Pr, Pb, Bi, U, As, Al, S, Ti, V, Cr, Mn, Fe, Co, Cu, Zn, Li and K) using the Climate Change Institute (CCI) Thermo Electron Element2 ICP-SFMS coupled to a Cetac Model ASX- 260 autosampler. The interferences were minimized by using an ESI Apex desolvating sample introduction system. All samples from the top 6 meters of the core and every 10th sample from the rest of the core were analyzed for stable water hydrogen and oxygen isotopes. The stable water isotope samples are reported as per mille relative to SMOW. They were analyzed as vapor on a Picarro Laser Cavity Ringdown Spectrometer (Model L2130-i) with a high throughput vaporizer. Detection limit for major and trace elements, and major ions (defined as three times the standard deviation of MilliQ (>18.2 MΩ) deonized water blanks passed through the entire continuous melting system) are shown in Table 2.1.

2.2 Dating of the ice core

The South Pole ice core record was annually dated, using a CCI software package [*Kurbatov et al.*, 2005], by matching seasonal peaks from Na, Sr and Cl^- (Figure 2.1A) and identification of major historical volcanic eruptions (Figure 2.1B). Peaks in Na and Cl^- concentrations in Antarctic ice cores are observed to occur primarily in winter/spring due to more intense atmospheric circulation and transport at this time [*Legrand and Mayewski*, 1997]. We found that Sr in the South Pole record also exhibits a well-defined seasonal signal, peaking in winter/spring similar to Na and Cl^- (Figure 2.1A), so it can also be used for annual layer counting. Major historical volcanic events, such as the 1963 CE Agung, 1883 CE Krakatoa, and 1815 CE Tambora eruptions, identified by large peaks in S and SO_4^{2-} concentration, were used as absolute time horizons during timescale development (Figure 2.1B). Once we developed a preliminary timescale and established volcanic signal markers, we compared the pattern of volcanic signals in our record with the volcanic signal in the WAIS divide ice core record [*Sigl et al.*, 2013]. The WAIS divide ice core has a higher accumulation rate, therefore, the annual signal is better preserved and there is less of a chance to have missing layers. We chose the age of the volcanic events using the WAIS timescale and interpolated to our record accordingly. On the basis of our dating, the South Pole record covers the period from -66 to 1999 CE. Estimated dating errors are: for the period 1963-1999 CE - ±1 year; 1815-1963 CE - ±3 years; 1458-1815 CE - ±11 years; 1257-1458 CE - ±12 years; 232-1257 CE - ±24 years. Because of the absence of any known historical eruptions in the deeper section of the core, we were not able to estimate dating error before 232 CE.

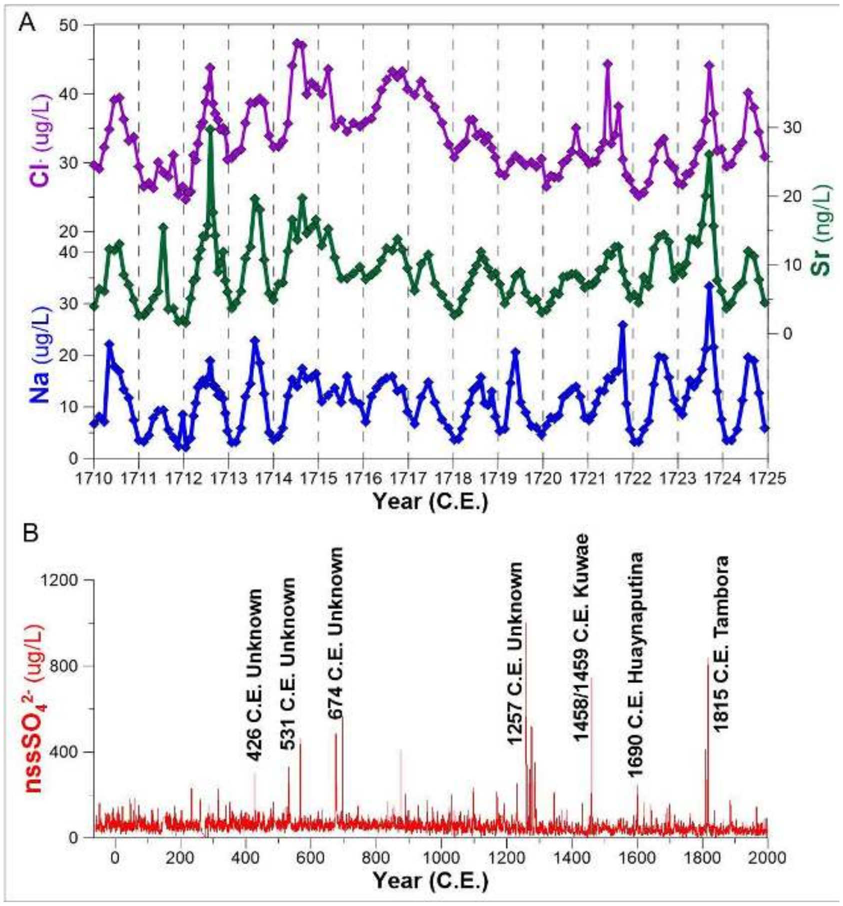

Figure 2.1 South Pole ice core timescale development. A) example of annual variations in Na (ug/L), Sr (ng/L) and Cl^- (ug/L) concentrations; B) $nssSO_4^{2-}$ record (ug/L) showing peaks attributed to major tropical volcanic eruptions.

Table 2.1 Method blanks and detection limits. Average method blank concentration (blank), method detection limit (MDL)[1], Mean, Minimum and Maximum South Pole sample concentrations, and a MDL-mean concentration comparison (MDLC)[2] for each element measured in this study.

			SPRESSO concentrations			
Element	Blank	MDL	Mean	Min	Max	MDLC (%)
Sr^{88}(LR) (ng/L)	0.22	0.04	14.73	< MDL	353.29	0
Cd^{111}(LR) (ng/L)	0.21	0.87	2.84	< MDL	302.62	31
Cs^{133}(LR) (ng/L)	0.05	0.01	0.27	< MDL	13.71	4
Ba^{138}(LR) (ng/L)	0.21	0.02	21.47	< MDL	3181.31	0
La^{139}(LR) (ng/L)	0.02	0.001	0.37	< MDL	30.36	0
Ce^{140}(LR) (ng/L)	0.01	0.001	0.77	< MDL	62.26	0
Pr^{141}(LR) (ng/L)	0.002	0.001	0.09	< MDL	7.08	1
Pb^{208}(LR) (ng/L)	0.18	0.002	7.57	< MDL	642.95	0
Bi^{209}(LR) (ng/L)	0.10	0.002	4.04	< MDL	869.52	0
U^{238}(LR) (pg/L)	3.77	0.05	86.78	< MDL	10874.30	0
As^{75}(LR) (ng/L)	0.19	0.13	1.82	< MDL	26.15	7
Li^{7}(LR) (ng/L)	0.39	0.24	5.94	< MDL	140.93	4
Al^{27}(MR) (µg/L)	0.33	0.47	4.59	< MDL	131.26	10
S^{32}(MR) (µg/L)	0.15	0.04	13.93	< MDL	361.88	0
Ca^{44}(MR) (µg/L)	0.08	0.01	2.95	< MDL	567.72	0
Ti^{47}(MR) (ng/L)	2.15	6.29	35.48	< MDL	2062.02	18
V^{51}(MR) (ng/L)	0.24	1.10	2.19	< MDL	284.34	50
Cr^{52}(MR) (ng/L)	0.16	0.15	24.31	< MDL	13290.24	1
Mn^{55}(MR) (ng/L)	3.06	10.38	33.64	< MDL	1848.05	31
Fe^{56}(MR) (µg/L)	0.08	0.00	0.83	< MDL	94.71	0
Co^{59}(MR) (ng/L)	0.77	2.12	24.14	< MDL	1522.82	9
Na^{23}(MR) (µg/L)	0.30	0.01	12.19	< MDL	413.51	0
Mg^{24}(MR) (ug/L)	0.65	3.34	10.29	< MDL	135.89	32
Cu^{63}(MR) (ng/L)	7.05	0.18	117.48	< MDL	3831.70	0
Zn^{66}(MR) (ng/L)	8.13	0.31	652.71	< MDL	31564.30	0
K^{39}(HR) (µg/L)	0.16	0.02	1.82	< MDL	298.95	1
Cl^{-} (µg/L)	3.15	2.26	31.16	< MDL	150.42	7
NO_3^{-} (µg/L)	6.73	4.82	84.67	< MDL	197.45	6
SO_4^{2-} (µg/L)	3.09	0.75	57.60	1.18	1002.89	1

[1] MDL is defined as three times the standard deviation of 5 MilliQ (>18.2 M?) deonized water blanks passed through the entire melter system

[2]MDLC = method detection limit as an approximate percentage of the mean ion or element concentration.

LR denotes low-resolution ICP-SMS mode (m/△m=300), and MR denotes medium-resolution mode (m/△m=4000)

CHAPTER 3

REORGANIZATION OF ATMOPSHERIC CIRCULATION BETWEEN 1400-1700 CE AS RECORDED IN A SOUTH POLE ICE CORE

3.1 Abstract

Here we present an ~2000 year high-resolution glaciochemical record from the South Pole. Significant changes in chemical concentrations, accumulation rate, stable water isotopes and deuterium excess records are demonstrated during the period ~1400-1700 CE, indicating a reorganization of atmospheric circulation that occurred in two steps: ~1400-1425 CE and ~1650-1700 CE. Major declines in dust and SO_4^{2-} concentrations are observed ~1400 CE suggesting poleward contraction and potential intensification of westerly air flow. The changes in stable water isotopes, deuterium excess, NO_3^- concentration and accumulation rate characterize a second shift in atmospheric reorganization between 1650-1700 CE indicating increased marine air mass intrusions and subsequent blocking of the katabatic winds, a colder (closer to the coast) moisture source for South Pole and a sea ice decrease in the Weddell Sea since ~1650-1700 CE.

3.2 Introduction

One of the major disturbances of the late Holocene climate is a cooling period in the Northern Hemisphere between ~1400-1850 CE, known as the Little Ice age (LIA) [*Jones and Mann*, 2004; *Matthews and Briffa*, 2005; *Mann et al.*, 2008, 2009; *Wanner et al.*, 2011]. The LIA was most likely caused by a combination of factors including: a decrease in solar activity, an increase in volcanic activity and a possible slowdown of the thermohaline circulation [*Mann et al.*, 2009; *Trouet et al.*, 2009; *Wanner et al.*, 2011; *Miller et al.*, 2012]. Several studies report evidence of a climate shift observed during a similar time interval in the Southern Hemisphere (SH) [*Mayewski et al.*, 2004a; *Moy et al.*, 2009; *Bertler et al.*, 2011]. Climate changes in the SH are, however, not homogenous, due to the regional differences in environment, climatology and ice dynamics over the vast expanse of Antarctica. A major climate driver in the SH is the Southern Hemisphere Westerlies (SHWs) belt. Intensity and position of the SHWs affect environmental conditions throughout Antarctica [*Mayewski et al.*, 2004b, 2009; *Shulmeister et al.*, 2004; *Bertler et al.*, 2011; *Dixon et al.*, 2012; *Sime et al.*, 2013] Several records from Antarctica and South America suggest a shift in atmospheric circulation and position of the SHWs sometime between 1300-1800 CE, however, they differ in their interpretations of the climate conditions and position and strength of the SHWs.

Moy et al. [2009] suggest an intensification and poleward shift of the SHWs and overall colder conditions in southern South America, based on several paleoclimate records from Patagonia. Moreno et al. [2009] show that the SHWs may have achieved its modern state at the beginning of the Little Ice Age, i.e. 570 years ago. Lechleitner et al. [2017] note a pronounced southward shift of the intertropical convergence zone (ITCZ) between 1320-1820 CE. Ceppi et al. [2013] show that the ITCZ tends to shift together with the SHWs, thus a southward shift in ITCZ during the LIA would coincide with a southward shift in the SHWs. Based on ice core records from Siple Dome, Mayewski et al. [2013] suggest a contraction and southward shift of the SHWs and displacement of ASL closer to coastal West Antarctica ~1600 CE. Kreutz et al. [1997] show an increase in meridional atmospheric circulation intensity in the polar South Pacific at the beginning (~1400 CE) of the LIA. Law Dome records show generally lower temperatures during the period 1350-1800 [*Ommen and Morgan*, 1997] . A study from Stenni et al. [2011] reports colder conditions during the LIA in Northern Victoria Land, East Antarctica. *Bertler et al.* [2011] published a summary of climatic changes during the LIA (1300-1800 CE) in Antarctica, suggesting overall cooler conditions during this period, with increased meridional circulation and strength of the SHWs winds, and increased sea ice production in the Ross Sea.

Other records suggest expansion and weakening of the SHWs during the LIA. A study using climate-proxy data from peat bogs reports drier conditions in Tierra del Fuego, southern South America, during the LIA which the authors attribute to the equatorward shift of the mean position of the SHWs [*Chambers et al.*, 2014]. Varma et al. [2012], using climate models and marine sediment records from the Chilean continental slope, note that during periods of low solar activity (such as Maunder Minimum) the SHWs become weaker near Antarctica and the belt expand equatorward. Based on a West Antarctic ice core record, Koffman et al. [2014] suggest that SHWs occupied a more southerly position during the Medieval Climate Anomaly (1050-1400 CE) and shifted northward at ~1430 CE. Meyer and Wagner [2008, 2009], show a northward shift of the SHWs during the LIA, based on both proxy records from South America and climate modeling studies.

Given the sometime conflicting results of previous studies as to the inferred atmospheric circulation during major climate events such as LIA, in this paper, we present a 2000 year ice core record from the South Pole that shows a shift in several glaciochemical parameters (SO_4^{2-}, NO_3^-, Ti, La, Ce, Pr, $\delta^{18}O$, δD and d-excess) indicating a major reorganization of atmospheric circulation between 1400-1700 CE.

3.3 Methodology

Ice core processing, chemical analyses, and timescale development are described in Chapter 2.

3.4 The South Pole ice core site

The South Pole is located in central Antarctica at an elevation of 2835 m a.s.l. (Figure 3.1). The prevailing wind direction at the South Pole is from north to east grid, emanating from the high interior of the East Antarctic plateau [*Lazzara et al.*, 2012]. These air masses have low concentrations of aerosols, because of the long distances the particles travel from their sources [*Hogan et al.*, 1982]. Proximity of the South Pole to the lower-altitude West Antarctic ice sheet means that South Pole also can be influenced by warmer and more moist air-masses entering West Antarctica from the south-east South Pacific or south-west South Atlantic oceans. South Pole Plateau receives warmer surface air and stronger surface winds than most of the Antarctic interior [*Hogan*, 1997]. Previous studies show that aerosols and particles are usually transported to the South Pole by these warm marine air mass intrusions occurring via Weddell, Amundsen-Bellingshausen and Ross Seas [*Bodhaine et al.*, 1986; *Shaw*, 1988; *Hogan and Gow*, 1993].

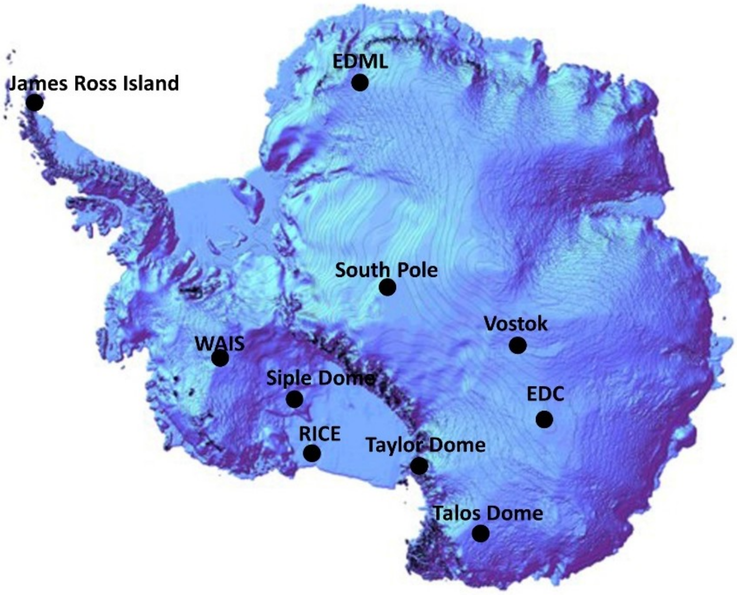

Figure 3.1 Map of the ice core location used in this study.

3.5 South Pole glaciochemical records.

A number of glaciochemical records, including stable isotopes, d-excess, SO_4^{2-}, NO_3^-, Ti, La, Ce, Pr, and accumulation rate, were chosen for this study to evaluate climate conditions for the past ~2000 years (Figure 3.2 and Table 3.1).

Table 3.1 Mean values of South Pole time series during different periods.

	60 BCE - 400 CE	400 CE - 650 CE	650 CE -1400 CE	1400 CE -1650 CE	1650 CE - 1998 CE
La (ng/L)	0.74	0.34	0.70	0.30	0.31
Ce (ng/L)	1.42	0.61	1.33	0.68	0.70
Pr (ng/L)	0.20	0.07	0.17	0.08	0.07
Ti (ng/L)	54.55	36.49	64.16	37.57	27.66
NO_3^- (ug/L)	81.28	88.01	91.26	83.87	74.05
SO_4^{2-} (ug/L)	63.32	66.52	62.65	46.29	43.52
δO^{18} (‰)	-50.23	-50.33	-50.54	-50.06	-48.72
δD (‰)	-404.69	-406.05	-406.19	-403.47	-393.79
d-excess	-2.82	-3.38	-1.86	-2.97	-4.08

3.5.1 Dust records

The dust signal in the South Pole record is represented by several elements: Ti, La, Ce, and Pr. All of these elements are highly correlated to each other and have very low crustal enrichment factors, indicating that the primary source for these elements is crustal dust. Figure 3.2 shows Ti variability for the past ~2000 years (note that other dust elements show similar variability as shown in Figure 3.3). The most elevated dust concentrations are observed until ~1400-1425 CE, except for the ~400-550 CE interval, when some of the dust elements show a decline in concentration (Table 3.1). The most significant shift in South Pole dust influx occurs ~1425 CE, when dust elements concentrations decrease ~1.5 times.

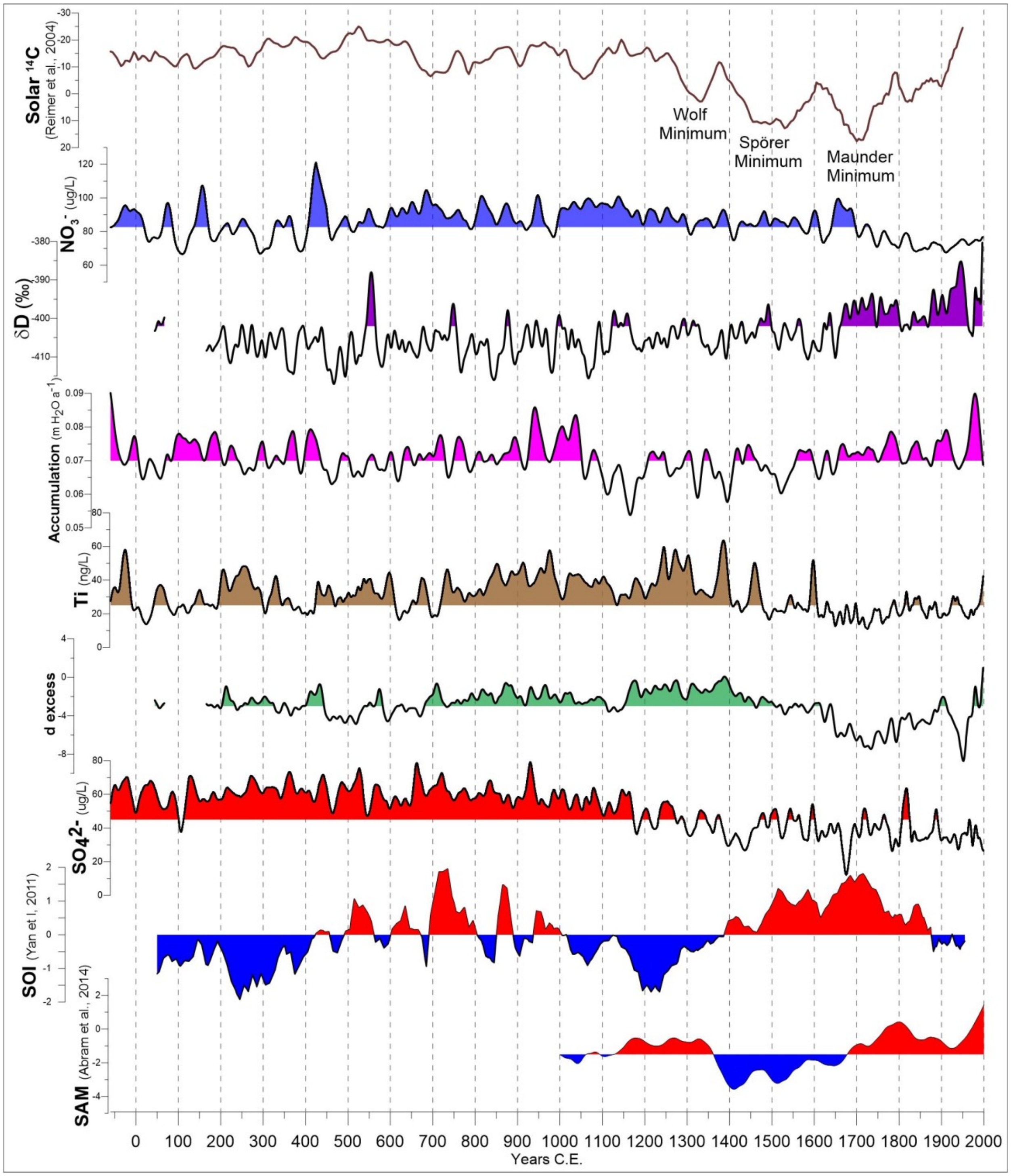

Figure 3.2 South Pole glaciochemical records. Also shown SOI [*Yan et al.*, 2011], SAM [*Abram et al.*, 2014] and solar irradiance [*Reimer et al.*, 2004] reconstructions.

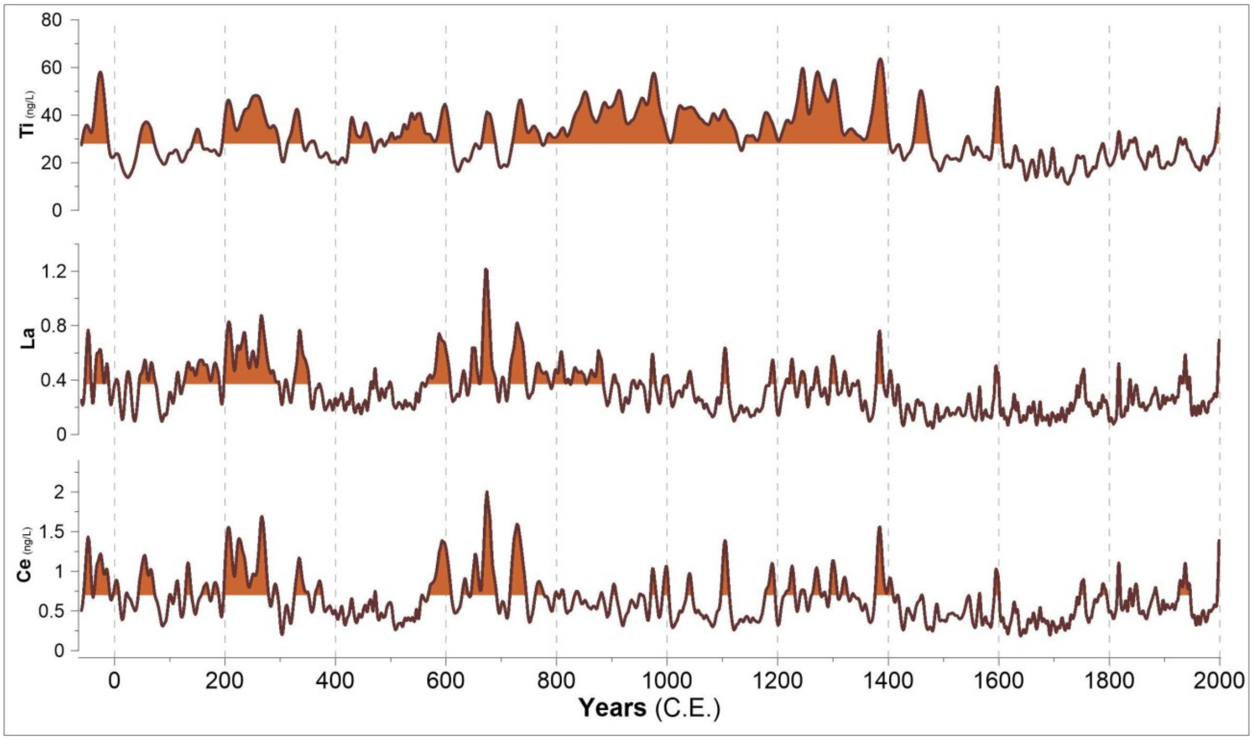

Figure 3.3 South Pole dust records.

Dust is transported to the Antarctic from the Southern Hemisphere lower-latitude landmasses by the SHWs. The observed decrease in dust deposition at ~1425 CE could be caused by changes in strength, latitude extent, and pattern (zonal vs meridional) of the SHWs. Figure 3.4 shows that during the period 1958-1998 South Pole Ti is positively correlated with the strength of the zonal near-surface winds. The positive correlation suggests that a decrease in dust concentrations since 1425 CE is related to weakening of the SHWs. A weakening of the SHWs during the LIA is supported by Varma at al. [2012] and suggested to be related to reduced solar irradiance. However, the period for which the correlation in Figure 3.4 is calculated is not very long. Moreover, one cannot assume that the same relationships between South Pole dust and zonal wind persisted in the past under potentially different climatic conditions. Several studies, in fact, show intensified westerly flow during LIA [*Kreutz et al.*, 1997; *Shulmeister*, 1999; *Mayewski et* *al.*, 2004a; *Moy et al.*, 2009; *Bertler et al.*, 2011]. Several studies [*Shulmeister*, 1999; *Mayewski et al.*, 2004a; *Goodwin et al.*, 2012] suggest domination of more intense westerly circulation during the LIA and more meridional circulation before the LIA. With more intense meridional flow, dust could be more easily transported to the South Pole, which could explain the elevated dust levels until ~1425 CE. An increase in zonal flow could lead to blocking of the Antarctic interior and thus cause a decrease in dust concentration noted in the South Pole records during the LIA.

Dust deposition at the South Pole is likely also related to the position of the SHWs. Most of the dust deposited in Antarctica originates from South America and Australia with the southern South American dust source being more significant for the South Pole region [*Li et al.*, 2008; *Neff and Bertler*, 2015]. The most southern major dust sources are in Patagonia (between 38-48°S), in the region under the influence of the SHWs [*Prospero et al.*, 2002; *Li et al.*, 2008]. Maximum dust activity in Australia is centered on the northeast side of present-day Lake Eyre [*Prospero et al.*, 2002]. Australian dust sources are located farther north, so transport of Australian dust to the South Pole would be possible during equatorward expansion of the SHWs. Our dust records suggest that before ~1425 CE the SHWs occupied a more northerly position because concentrations are higher, therefore, involving dust from Patagonia and possibly also Australia. The major decrease in dust deposition ~1425 CE could be a result of contraction and poleward shift of the SHWs, thus decreasing the dust source areas exposed to the SHWs. Several studies, based on proxy records from Antarctica, South America and Australia, also suggest a poleward shift of the SHWs during the LIA [*Shulmeister et al.*, 2004; *Moreno et al.*, 2009; *Moy et al.*, 2009; *Mayewski et al.*, 2013]. Other studies, however, argue that SHWs shifted north during the LIA [*Meyer and Wagner*, 2009; *Varma et al.*, 2012; *Chambers et al.*, 2014; *Koffman et al.*, 2015].

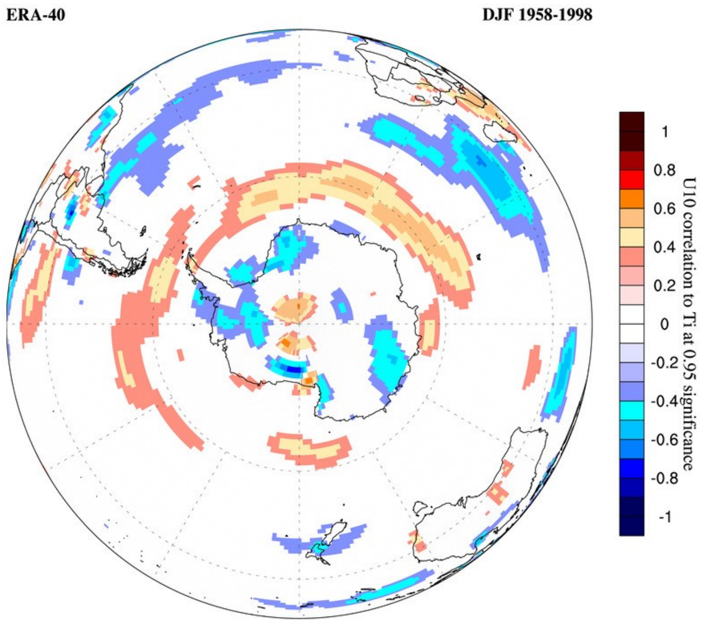

Figure 3.4 Correlation between South Pole Ti data and surface wind at 10 m (U10) for the period 1958-1998 CE. Correlations were made with ECMWF 40-year reanalysis (ERA-40) data using Climate Reanalyzer (https://ClimateReanalyzer.org), Climate Change Institute, University of Maine, USA.

Lowered dust concentrations can also be related to changes in precipitation, such that increased precipitation would lead to dust being precipitated out en-route and not reaching South Pole. Our records do not show any evidence for a precipitation increase at ~1425 CE. However, our records show an increase in accumulation rate and stable water isotopes ~1650 CE, which indicates an increase in precipitation and might at least partially account for the lower dust levels during LIA.

3.5.2 SO_4^{2-}

The most elevated SO_4^{2-} values are noted until ~1175 CE, after which time SO_4^{2-} concentration starts to decline. The most pronounced decrease is observed ~1400 CE, shortly preceding the decrease in dust concentrations (Figure 3.2, table 3.1).

Except for brief intervals during large volcanic eruptions, the major natural source for SO_4^{2-} in Antarctica is marine biogenic emission [*Mayewski et al.*, 1990; *Legrand and Mayewski*, 1997]. SO_4^{2-} comes from the oxidation of dimethylsulphide (DMS) produced by marine phytoplankton and emitted from the ocean surface [*Legrand et al.*, 1991; *Minikin et al.*, 1998]. Increased oceanic emission of DMS characterizes glacial intervals due to an increase in sea ice extent [*Welch et al.*, 1993; *Wolff et al.*, 2006].

The South Pole ice core record reveal a decrease in SO_4^{2-} concentrations after ~1400 CE. This could imply a decrease in the production of biogenic sulfate, potentially related to a decrease in sea ice extent or a shift in atmospheric transport of SO_4^{2-} to interior Antarctica. Variation in snow accumulation may also affect concentrations of sulfate in snow, however, we do not see any correlation between SO_4^{2-} and accumulation in our record. Our South Pole SO_4^{2-} record shows positive correlation with sea ice extent during austral spring in the Weddell Sea and Indian sector of the Southern Ocean, and negative correlation with parts of the Ross Sea for the period 1979-1998 CE (Figure 3.5). Bertler et al. [2011] show an increase in sea ice during the LIA in the Ross Sea. Based on the dipole response of the Ross and Weddell Seas to climate forcing [*Carleton*, 2003; *Lefebvre and Goosse*, 2005] (Figure 6), one would expect a decrease in sea ice during the LIA in the Weddell Sea. We suggest that the decrease in South Pole SO_4^{2-} indicates a decrease in sea ice extent in the Weddell Sea and potentially in the Indian sector of the Southern Ocean since ~1400 CE. A decrease in sea ice extent and therefore larger amount of open water source is also suggested by changes in South Pole isotopic values discussed below.

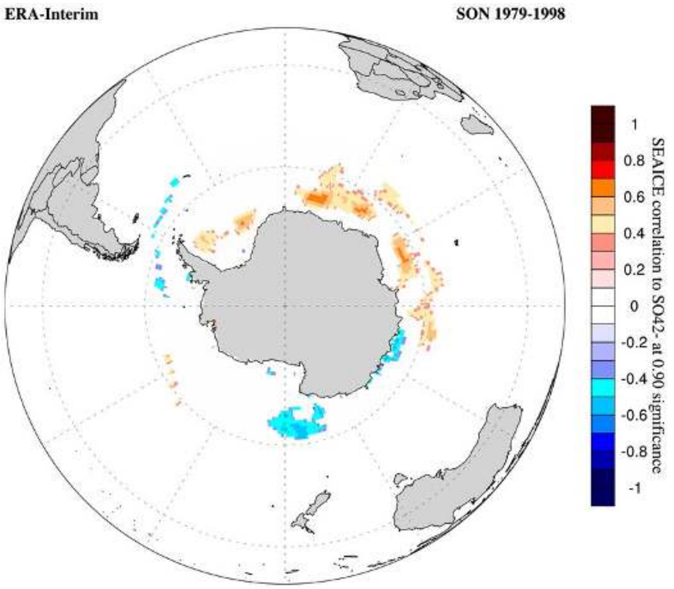

Figure 3.5 Correlation between South Pole SO_4^{2-} data and sea ice concentration during SON for the period 1979-1998 CE. Correlations were made using European Reanalysis Interim (ERA-Interim) data from Climate Reanalyzer (https://ClimateReanalyzer.org), Climate Change Institute, University of Maine, USA.

The decrease in SO_4^{2-} during LIA corresponds to the major decline in dust concentration, and as discussed earlier could be related to the change to a more zonal atmospheric circulation. Unlike coastal Antarctic sites, South Pole SO_4^{2-} typically shows a maximum concentration during winter/spring (together with Cl^-), suggesting that biogenic SO_4^{2-} is transported from more distant northerly located areas by winter/spring storms. A decline in SO_4^{2-} concentration since 1400 CE therefore could be caused by a contraction of the polar vortex and subsequent decrease in transport of SO_4^{2-} from distant ocean sources.

3.5.3 Stable water isotopes

The oxygen and hydrogen isotopic composition of polar ice is used to obtain paleoclimate information, such as past local surface temperature changes at the precipitation site [*Petit et al.*, 1999]. Our South Pole isotope records show a weak correlation to Amundsen-Scott station air temperature (Figure 3.6). This weak correlation might be attributable to dating uncertainty and lack of an annual isotopic signal in the South Pole record. The latter could be explained by the fact that South Pole ice core was stored in a freezer facility for a few years before it was sampled, and the long storage period might have caused smoothing of the isotopic signal [*Jouzel*, 2003].

Figure 3.2 shows the δD record for the last ~2000 years. South Pole $\delta^{18}O$ and δD values are relatively stable until ~1650 CE, except for a short-term increase around 550 CE. A slightly elevated base level is observed for the period 1100-1650 CE compared to earlier times. The most significant shift in water isotopes occurred ~1650 CE, when $\delta^{18}O$ and δD values increase by ~3% compared to the earlier interval. Our records demonstrate that this shift was rapid, occurring in less than a decade.

Stable isotope variability in ice core records is linked to changes in cyclonic activity around Antarctica [*Ekaykin et al.*, 2004]. An increase in cyclonic activity results in more precipitation and warmer temperatures [*Morgan et al.*, 1991; *Ekaykin et al.*, 2004]. Therefore, we interpret the increase in stable isotopes since ~1650 CE as an increase in the penetration of warm marine air masses to the South Pole produced by an increase in cyclonic activity.

Figure 3.6 shows stable water isotopes from other Antarctic sites revealing the large spatial and temporal climatic variability. Several ice core records show a decrease in stable isotope values during the LIA. Victoria Lower Glacier (VLG) shows cooling between 1300-1800 CE with the transition to colder conditions occurring rapidly, in less than a decade [*Bertler et al.*, 2011]. Talos Dome shows slight cooling since ~1450 CE, accompanied by an increase in accumulation [*Stenni et al.*, 2011]. Taylor Dome reveals cooling between 1400-1800 [*Steig et al.*, 2000]. The WAIS ice core indicates gradual cooling in central West Antarctica during the last 1000 years [*Fudge et al.*, 2013]. EPICA Dome C from East Antarctica indicates cold conditions 1400-1800 CE [*Jouzel et al.*, 2007]. In contrast, several other records show an increase in isotope values during the last few centuries. RICE, in West Antarctica shows warmer conditions since 1450 CE [*RICE community members*, 2018]. Located nearby, Siple Dome also suggests warmer conditions [*Brook et al.*, 2005; *Fudge et al.*, 2013]. Records from the Antarctic Peninsula demonstrate warming after ~1700 CE [*Abram et al.*, 2014]. Our records indicate that the South Pole climate is different from that at East Antarctic sites and also from the interior of West Antarctica. It shows more similarity with the isotopic changes in the Antarctic Peninsula. South Pole is most likely representing the most interior intrusion of air masses coming from the Weddell and Bellingshausen Seas.

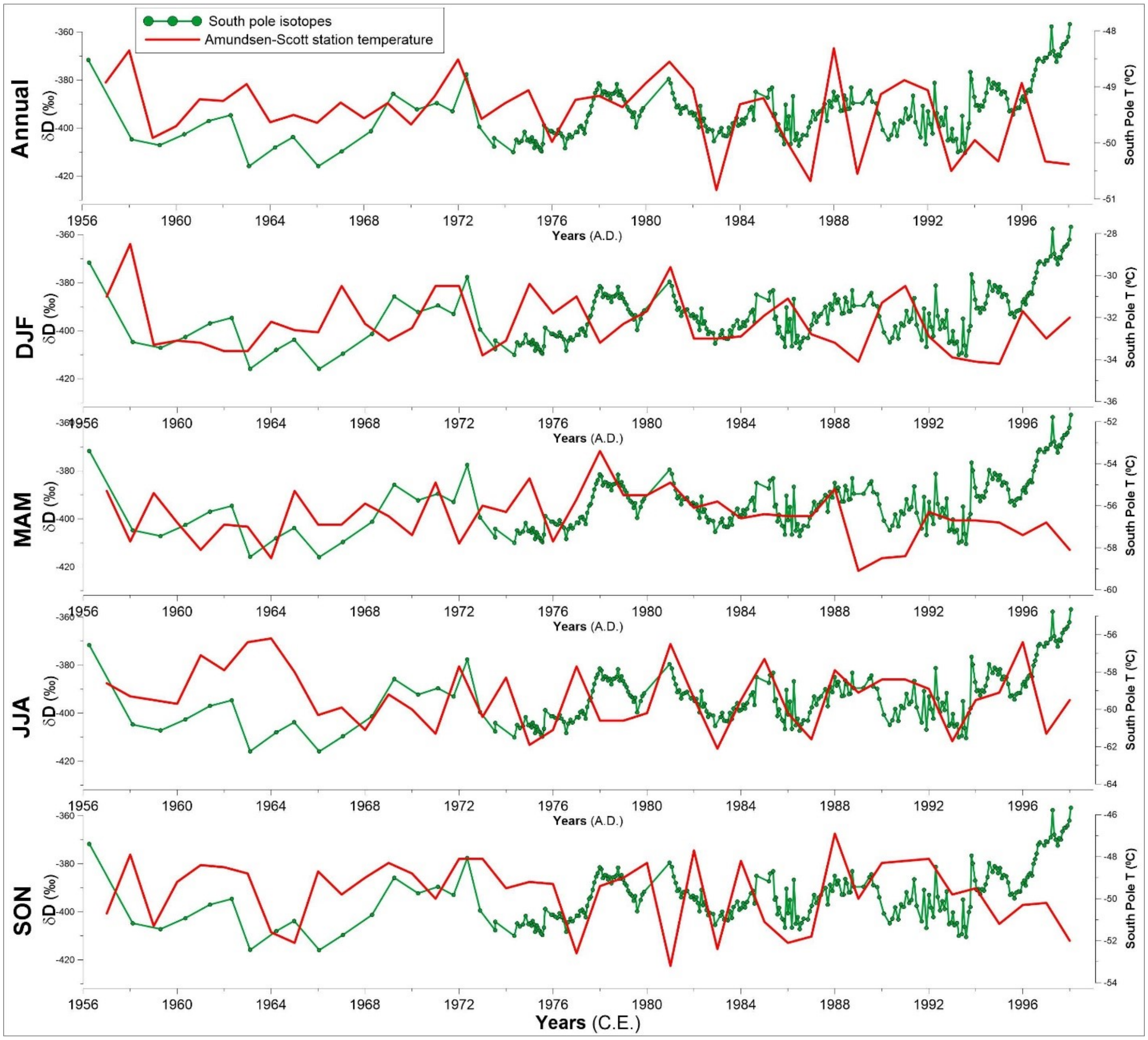

Figure 3.6 Comparison between South Pole stable water isotopes and Amundsen-Scott temperature records. Amundsen-Scott station temperature records are from https://legacy.bas.ac.uk/met/READER/surface/Amundsen_Scott.00.temperature.html

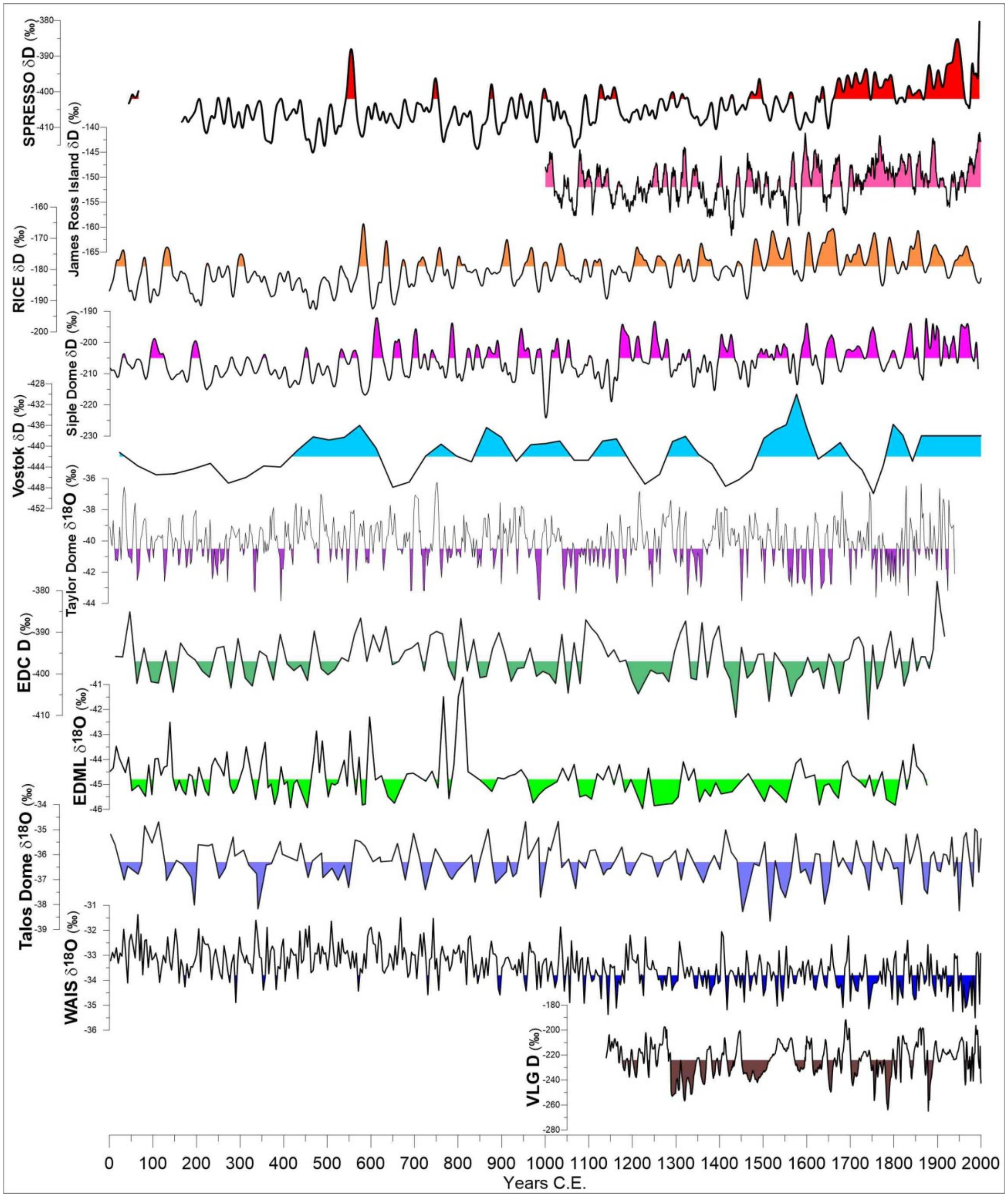

Figure 3.7 Antarctic stable water isotope records. Stable water isotopes data from top to bottom: South Pole (this study), James Ross Island [*Abram et al.*, 2014], RICE [*RICE community members*, 2018], Siple Dome [*Brook et al.*, 2005; *Fudge et al.*, 2013], Vostok [*Petit et al.*, 1999], Taylor Dome [*Steig et al.*, 2000], EDC [*Jouzel et al.*, 2007], EDML [*Barbante et al.*, 2006], Talos Dome [*Stenni et al.*, 2011], WAIS [*Fudge et al.*, 2013], and VLG [*Bertler et al.*, 2011].

3.5.4 Deuterium excess

Deuterium excess ($d=\delta D-8\times\delta^{18}O$) is a second-order isotopic parameter used to assess moisture source [*Vimeux et al.*, 2001]. There are two major factors controlling d-excess: ocean surface temperature (SST) during evaporation and relative humidity at the vapor source region. d-excess is in general positively correlated with SST, and anticorrelated with relative humidity [*Jouzel et al.*, 2013; *Pfahl and Sodemann*, 2014].

The South Pole mean d-excess value is ~ -2.9 ‰ (varying from +3.7 to -25.9 ‰). Previous studies show that negative d-excess values are observed in ice core sites with elevations lower than 2000 m. The differences in d-excess between low and high elevation sites suggest different moisture source regions, where low elevation and coastal locations receive moisture from the colder high-latitude ocean; and interior Antarctic sites having elevations above 2000 m receive moisture from the subtropics and mid-latitudes [*Masson-Delmotte et al.*, 2008; *Sodemann and Stohl*, 2009]. The more negative South Pole d-excess values suggest that the South Pole receives precipitation from a more southerly located region than do the more interior areas of East Antarctica.

The d-excess at the South Pole is shown in Figure 3.2. South Pole d-excess values stay relatively high between 50-1500 CE, except for a minor decrease between ~450-670 CE. The highest values are observed between 700 and 1450 CE, indicating warmer SST and lower humidity at the moisture source. The d-excess values start to decline after 1450 CE, followed by a sharp decrease at ~1650 CE, suggesting a decrease in SST and increased humidity at the moisture source, or a shift to a colder higher latitude moisture source. Similar to $\delta^{18}O$ and δD, changes in d-excess occur abruptly, over about 10 years, in the South Pole record. The South Pole d-excess values reach a minimum at ~1725 CE, then start to rise slowly, except for a sharp drop ~1950 CE.

3.5.5 NO_3^-

The presence of NO_3^- in Antarctic ice cores is attributed to a variety of sources such as tropospheric lightning, NOx produced from N_2O oxidation in the lower stratosphere, galactic cosmic rays and/or surface sources such as biomass burning and NO exhalations from soils [*Legrand and Kirchner*, 1990]. Nitrate concentrations in Antarctic snow are also be linked to the extent and/or persistence of polar stratospheric clouds (PSCs) (Mayewski and Legrand, 1990; Mayewski et al., 1995). NO_3^- is transported mostly through the upper troposphere and stratosphere from distant sources [*Legrand and Kirchner*, 1990; *Mayewski et al.*, 2005]. NO_3^- concentration is also assumed to be related to temperature and accumulation rate, whereby lower temperatures lead to higher mean NO_3^- concentrations [*Legrand and Mayewski*, 1997] Rothlisberger et al., 2000).

South Pole NO_3^- concentrations exhibit elevated values for the period 60 BCE to ~1700 CE and a decrease from ~1700 CE (Figure 3.2, Table 3.1). The decrease in NO_3^-, in general, coincides with a major shift in stable water isotopes, suggestive of increased penetration of marine air masses to the South Pole. More frequent marine air intrusions would, in turn, reduce the katabatic transport of air from the Antarctic interior and subsequently lead to a decrease in deposition of NO_3^- at the South Pole.

3.6 Influence of SAM and ENSO teleconnections, and solar activity on South Pole climate variability.

The Southern Annual Mode (SAM) is the dominant pattern of climate and atmospheric variability in the Southern Hemisphere [*Marshall*, 2003b; *Abram et al.*, 2014], and is a measure of the position and strength of the SHWs. Positive SAM is associated with intensification and poleward shift of the SHWs, and low-pressure anomalies over Antarctica compared to midlatitudes [*Swart et al.*, 2015]. Figure 3.2 shows SAM reconstruction for the last millennium based on Antarctic temperature proxy records [*Abram et al.*, 2014].

Another major atmospheric circulation feature in the Southern Hemisphere is the tropical El Niño Southern Oscillation (ENSO). We use proxy-based reconstructions of the Southern Oscillation Index (SOI) for the past 2,000 years [*Yan et al.*, 2011] to show ENSO variability and change (Figure 3.2). The SOI index is based on the difference of mean sea level pressure between Tahiti (17.5°S, 149.6°W) and Darwin, Australia, (12.4°S, 130.9°E). Negative SOI anomalies indicate El Niño like conditions and positive SOI indicate La Niña dominated conditions.

Previous studies demonstrate that polar/tropical teleconnections are stronger for +SAM/La Niña and -SAM/El Niño combinations, or when ENSO events occur with weak SAM [*Fogt et al.*, 2011]. The La Niña influence on climate in the SH is very similar to the influence of +SAM. Figure 3.8 shows the correlation between ENSO (represented by SOI index), SAM and several climate parameters using ERA-Interim climate reanalysis data. Positive SAM coupled with a La Niña like climate is characterized by deepening of the Amundsen Sea Low (ASL), intensification and contraction of the SHWs, increased precipitation and warming over Antarctic Peninsula and parts of West Antarctica, cooling over most of East Antarctica, decreased sea ice extent in the Weddell/Bellinsgausen Seas, and increased sea ice in Ross/Amundsen Seas. ENSO reconstruction show La Niña dominated conditions during LIA, with a more pronounced shift to the negative ENSO ~1600 CE (Figure 3.2). The SAM reconstruction shows the most negative values ~1400 CE with a positive trend after that (Figure 3.2).

Previous studies show that South Pole climate is affected by both SAM and ENSO variations [*Meyerson et al.*, 2002; *Lazzara et al.*, 2012]. We compare 25-year resampled South Pole glaciochemical data with SAM and ENSO reconstructions to investigate their long-term association (Table 3.2). Our results show a significant positive correlation between SAM and stable water isotopes, and a significant negative correlation between NO_3^- and d excess (Table 3.2). Increase in isotopes and a decrease in d-excess and NO_3^- concentrations are associated with a trend to more +SAM since ~1650 CE (Figure 3.2).

Variations in ENSO have a more pronounced influence on South Pole records. Table 3.2 shows a significant negative correlation between SOI and d-excess, SO_4^{2-}, dust, and NO_3^- concentrations; and a positive correlation with stable water isotopes. Decreases in South Pole dust and SO_4^{2-} concentrations coincide with the shift to La Niña dominated conditions ~1400 CE based on SOI reconstruction. The shift in South Pole water isotopes, accumulation, and NO_3^- records ~1650-1700 CE coincides with a maximum SOI values at that time. Our records, however, do not show any major changes during the period from 60 BCE to ~1400 CE and suggest relatively stable El- Niño dominated conditions prior to ~1400 CE.

Table 3.2 Correlation between 25-years resampled South Pole glaciochemical data and SAM, SOI and solar activity reconstructions. Statistically significant positive/negative correlations ($p<0.1$) are highlighted in yellow/blue. Correlation with SAM reconstruction [*Abram et al.*, 2014] covers last ~1000 year interval, correlations with SOI [*Yan et al.*, 2011] and solar activity reconstruction [*Reimer et al.*, 2004] cover last ~2000 years.

	SAM	**SOI**	**Solar ^{14}C**
La	0.09	-0.19	-0.29
Ce	0.10	-0.33	-0.30
Pr	0.09	-0.39	-0.32
Ti	-0.09	-0.26	-0.19
NO_3^-	-0.39	0.07	-0.09
SO_4^{2-}	0.17	-0.26	-0.38
$\delta^{18}O$	0.35	0.25	0.27
δD	0.33	0.17	0.23
d_{ln}	-0.32	-0.41	-0.29
Accumulation	0.22	0.14	0.04

We also investigated the potential influence of changes in solar activity on our South Pole glaiochemical time series. Mayewski et al. [2005] show increased zonal wind strength near the edge of the polar vortex (40-50ºS) during intervals of increased solar activity. Varma et al. [2012], using model output and marine sediment records from the Chilean continental slope, suggest that during periods of low solar activity (Maunder Minimum) the SHWs weaken near Antarctica and expand north, towards the equator. Figure 3.2 shows a total solar irradiance (TSI) reconstruction based on tree-ring ^{14}C measurements [*Reimer et al.*, 2004].

Table 3.2 shows that South Pole dust elements, SO_4^{2-} and d-excess are negatively correlated, and stable water isotopes are positively correlated with solar activity. The correlations suggest that periods with lower solar activity, like the Maunder Minimum during LIA, are characterized by more positive ^{14}C values, South Pole sees a decrease in the dust, SO_4^{2-} and d excess values, and more positive isotope values.

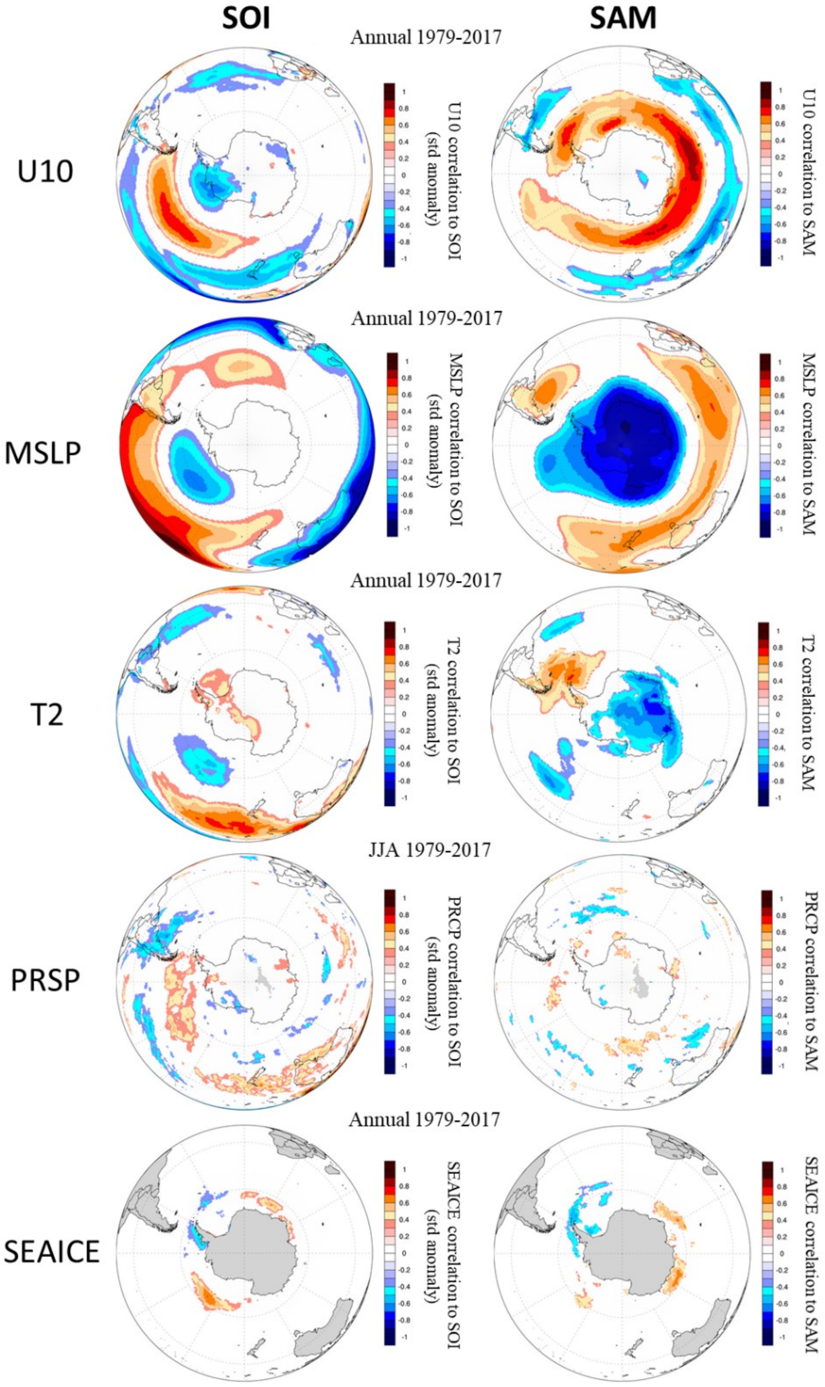

Figure 3.8 Correlation between SAM, SOI and climate parameters. Correlations are shown between SAM and SOI indexes and surface westerly wind at 10 m (U10), mean sea level pressure (MSLP), surface temperature (T2), precipitation (PRCP), sea ice concentration (SEAICE) for the period 1979-2007 CE. Correlations were made using European Reanalysis Interim (ERA-Interim) data from Climate Reanalyzer (https://ClimateReanalyzer.org), Climate Change Institute, University of Maine, USA. All correlations are at 0.95 significance.

3.7 Conclusions

This study presents an ~2000 year-long high-resolution glaciochemical record from the South Pole. The record reveals major changes during the period between 1400-1700 CE, corresponding to the initial and middle stages of the LIA. The most pronounced decrease in SO_4^{2-} is observed ~1400 CE. A significant decrease in dust elements concentrations occurs ~1425 CE. The d excess starts to decline after 1450 CE, followed by a sharp decrease at ~1650 CE. South Pole stable water isotopes show a shift to more positive values ~1650 CE, accompanied by an increase in the snow accumulation rate. The NO_3^- record shows a decrease in concentration ~1700 CE. Taken together, the South Pole records demonstrate a major reorganization of atmospheric circulation between ~1400-1700 CE.

Our South Pole glaciochemical records suggest that that atmospheric reorganization occurred in two major steps. The first shift in circulation occurred ~1400 CE, as evidenced by a decline in dust and SO_4^{2-}. We suggest that these decreases were the result of a poleward displacement and zonal intensification of the SHWs, thus restricting dust and SO_4^{2-} transport from the middle-latitudes to Antarctica. Changes in SO_4^{2-} possibly also indicate a decrease in winter-spring sea ice extent in the Weddell Sea during LIA, which was countered by an increase in the ice extent in the Ross Sea sector.

The second major shift in atmospheric circulation occurred ~1650-1700 CE, as evident by major changes in the stable water isotopes, d-excess, and NO_3^- records. This second shift is related to increased cyclonic activity and subsequent enhanced penetration of marine air masses to South Pole, displacement of the moisture source to a colder higher latitude ocean location, reduction of the katabatic air transport to the South Pole from the interior of East Antarctica, and a decrease in sea ice extent in Weddell Sea. The ~1650-1700 CE atmospheric shift may indicate a further contraction and intensification of the SHWs.

South Pole glaciochemical records show relatively stable climate conditions prior to onset of the LIA, except for the period ~450-650 CE. During this interval there is a slight decrease in dust concentration and more negative d-excess values, indicative of climate conditions similar to the LIA, but smaller in magnitude. In the Northern Hemisphere, this interval corresponds to a cold event between 400-765 CE, known as the Dark Ages Cold Period [*Wanner et al.*, 2011; *Helama et al.*, 2017].

Correlation of the South Pole ice core record with reconstructions of the SAM and ENSO show that both teleconnections have a strong influence on South Pole climatic conditions. In summary, our South Pole glaciochemical records show that prior to ~1400 CE the SH climate was dominated by El Niño-like conditions that changed to a +SAM/La Niña dominated climate conditions during the LIA.

CHAPTER 4

A 2000-YEAR RECORD OF ARSENIC VARIABILITY FROM A SOUTH POLE ICE CORE

4.1. Abstract.

Using a South Pole ice core covering the last ~2000 years we present a high-resolution (~9 samples/year), continuous record of natural and anthropogenic arsenic (As) deposition. Our results show that volcanic emissions (notably from Mt. Erebus) are a significant source of As for South Pole, and human activities most likely contributed to As deposition as early as 225 CE The most significant anthropogenic source As enrichment in the record, starting in 1975 CE, is linked to increased copper production in Chile and at least partially to coal combustion from throughout the Southern Hemisphere. East and West Antarctic ice core delivered deposition differences are a result of differences in the atmospheric circulation patterns that transport As to these regions.

4.2. Introduction

Arsenic is one of the most toxic elements in the environment and can be found in low concentrations throughout the geosphere. It can enter the environment through both natural processes and anthropogenic activities [*Chilvers and Peterson*, 1987; *Garelick et al.*, 2008]. Several studies report increases in As concentrations during the late 20th century in soil, water and air worldwide. In many cases elevated As is attributed primarily to human activities [*Bhattacharya et al.*, 2007; *Reimann et al.*, 2009]. The residence time of As in the atmosphere, between 7 and 10 days [*Matschullat*, 2000], allows As to be transported over relatively long distances. Ice core records provide an excellent opportunity to reconstruct the history of As concentrations in the atmosphere in remote regions**.** Atmospheric models show that air masses from South America, Australia and southern Africa can reach the Antarctic continent in ~10 days [*Li et al.*, 2010; *Albani* *et al.*, 2012; *Dixon et al.*, 2012; *Sudarchikova et al.*, 2015], therefore even the Antarctic continent is potentially impacted by pollution from Southern Hemisphere countries. Elevated concentrations of several trace elements (Pb, Cu, Cr, Zn, Ag, U and Bi) are documented in Antarctic ice core records and are attributed to emissions from smelting and mining operations, combustion of fossil fuel and use of leaded gasoline in Australia and South America [*Planchon et al.*, 2002b; *Hur et al.*, 2007; *Potocki et al.*, 2016]. Concentrations of As have been reported in a few Antarctic ice core records that cover the last 45-125 years, and it has been suggested that enrichment during the second half of the 20th century is attributed to increased copper smelting in Chile [*Hong et al.*, 2012; *Rong et al.*, 2016; *Schwanck et al.*, 2016]. Enrichment in As during the last 3000 years due to metallurgical activities in the Northern Hemisphere is reported in an ice core record from Devon Ice Cap in the Arctic [*Krachler et al.*, 2009]. Therefore, it is possible that human activities also affected atmospheric As deposition prior to the 20th century in the Southern Hemisphere.

Here we present a continuous high-resolution record of atmospheric As concentrations from a South Pole ice core for the period from 60 BCE to 1999 CE. The goal of this paper is to investigate As sources impacting Antarctica and to separate variability related to natural versus anthropogenic sources.

4.3 Methodology

A detailed description of core collection and processing, sample analysis, and timescale development are in Chapter 2. This study focuses on changes in As concentration in the South Pole ice core chemistry record. As concentrations were measured at low resolution (LR) mode. The LR mode is preferable for analyzing elements with very low concentrations, because of its higher sensitivity. Comparison with HR mode data shows that the LR data are not affected by potential As interferences (Figure 4.1). Detection limit for As is 0.27 ng/L (Table 2.1).

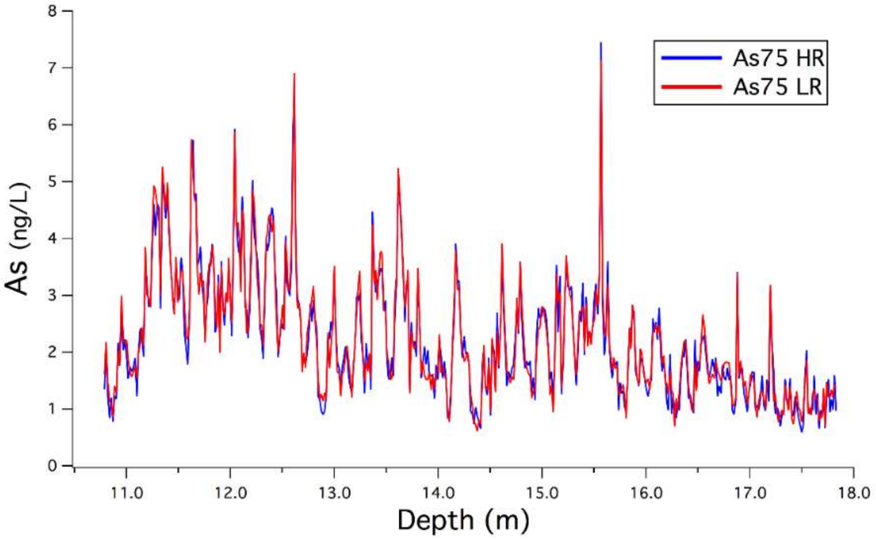

Figure 4.1 Comparison of As concentrations analyzed in low (LR) and high resolution (HR) ICP-SFMS modes.

4.4. Results and discussion

4.4.1 As concentrations for the period from 60 BCE to 1999 CE

Figure 4.2 shows the high-resolution (1-27 samples/year) record of As variability developed from the South Pole ice core. Concentrations of As in our record are low and vary from 0.27 to 26.15 ng/L, with an average concentration of 1.8 ng/L. Our South Pole As record exhibits several periods of increased concentration: ~225-325 CE, ~645-985 CE, ~1260-1400 CE, and ~1730-1999 CE (Table 4.1). The most significant increase in As concentrations is observed after 1975 CE, when concentrations average 6.6 ng/L, which is four times higher than during the period 60 BCE to 1974 CE.

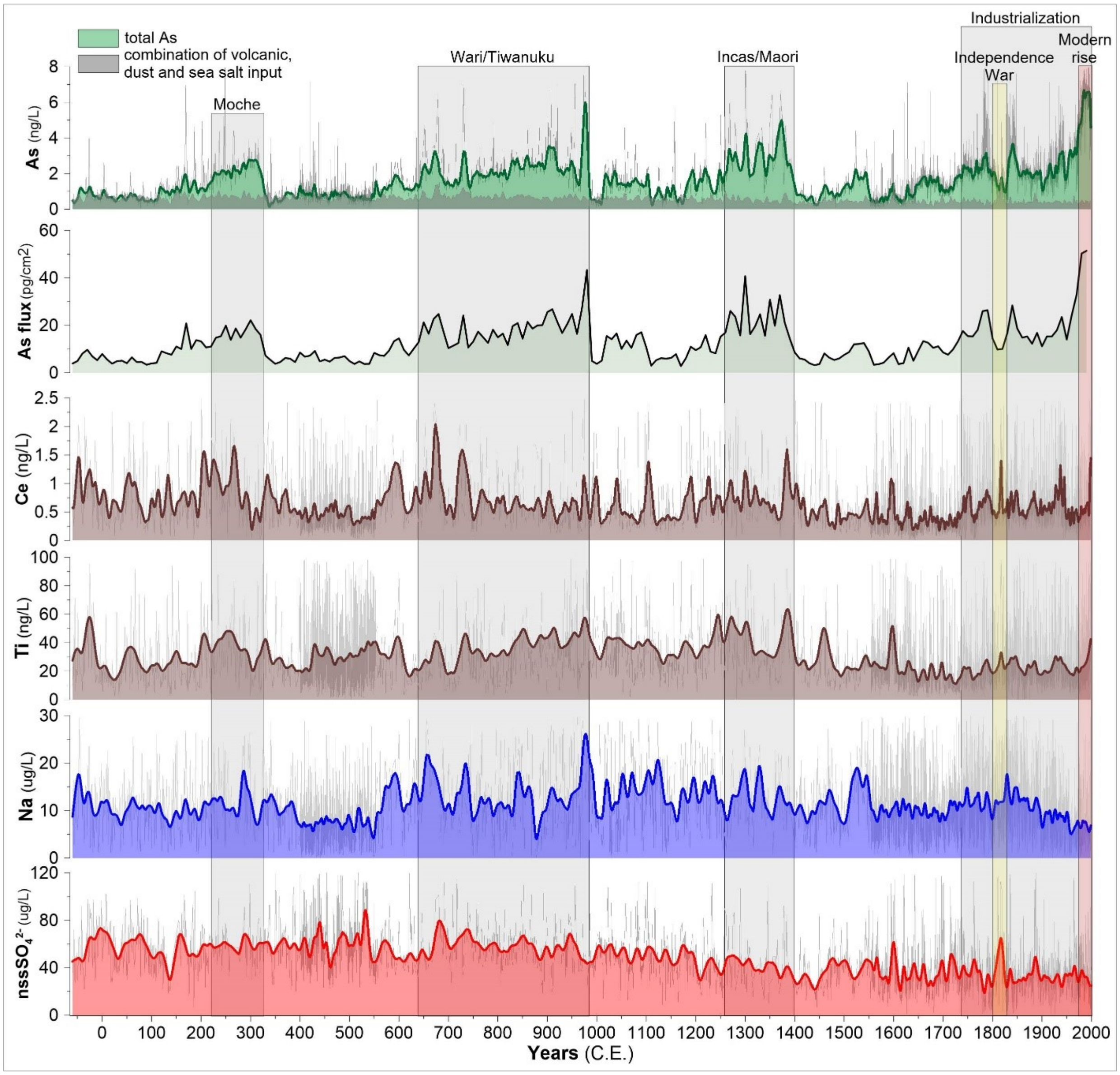

Figure 4.2 South Pole records of As variability. Time series from top: As (ng/L), As flux (pg/cm^2), Ce (ng/L), Ti (ng/L), Na (ug/L), and nssSO$_4^{2-}$ (ug/L) for the period from 60 BCE to 1999 CE. The light grey color lines show raw data. The colored lines represent background levels estimated using a robust spline smoothing function. Note that some raw values exceed the vertical scale. Flux is shown as 10-year resampled data. Colored horizontal bands define periods of changes in As concentrations related to anthropogenic activities.

As flux (concentration*annual accumulation rate) is also shown in Figure 4.2. Both As flux and As concentration demonstrate similar variability, indicating that the changes in As concentrations in South Pole records are not associated with changes in snow accumulation rate.

Table 4.1 Mean concentrations of South Pole As during different periods, and estimated contributions from natural sources and their percentage relative to the measured concentrations.

	As	**Sea spray**		**Volcanic**		**Soil dust**	
Periods with elevated As concentration:	**ng/L**	**ng/L**	**%**	**ng/L**	**%**	**ng/L**	**%**
225-325 CE	2.5	0.004	0.2	0.6	29.2	0.1	6.4
645-985 CE	2.5	0.006	0.2	0.6	29.2	0.1	6.2
1260-1400 CE	2.7	0.006	0.3	0.5	27.3	0.1	5.3
1730-1974 CE	2.4	0.005	0.2	0.4	21.7	0.1	3.1
1975-1999 CE	6.5	0.003	0.0	0.3	5.5	0.1	1.3
Periods with low As concentration:							
60 BCE-224 CE	1.0	0.005	0.5	0.5	80.1	0.1	12.7
326-645 CE	0.9	0.003	0.4	0.6	92.2	0.1	8.0
986-1259 CE	1.4	0.006	0.7	0.5	79.2	0.1	7.6
1401-1729 CE	1.1	0.004	0.5	0.4	59.7	0.0	5.0

4.4.2 Estimation of contribution from natural sources.

Arsenic can enter the atmosphere from several natural sources including: crustal and soil dust, sea salt aerosols, wild forest fires, volcanic and biogenic emissions [*Nriagu*, 1989]. Previous studies suggest that explosive volcanic eruptions and quiescently degassing volcanoes are the primary natural source for As [*Chilvers and Peterson*, 1987; *Nriagu*, 1989].

To evaluate the natural contribution to South Pole As, we calculated soil dust, sea salt spray and volcanic emission input. The sea salt spray contribution is calculated using the following equation:

$As_{sea\ salt}=Na_{sample}*([As/Na]_{ocean\ water})$,

where ocean elemental abundances are from Lide [2005].

The As contribution from soil dust is calculated using the following equation:

$As_{soil\ dust}=X_{sample}*([As/X]_{soils})$,

where X is a reference element and concentrations of elements in soils are from *Kabata-Pendias* [2011]. We estimated a mean soil dust contribution using Ti, Pr, La and Ce as reference elements.

Our source partitioning calculations show that the sea spray contribution is negligible (<1%) throughout the whole record (Table 4.1). This is similar to previous estimations and other observations in Antarctic records [*Chilvers and Peterson*, 1987; *Hong et al.*, 2012; *Schwanck et al.*, 2016]. Contributions from soil dust are also small and on average account for ~5% of total As (Table 4.1).

Contributions from quiescent volcanic degassing are calculated using SO_4^{2-} concentrations in South Pole samples and mean values of As/S ratios in volcanic emissions. We assume that 2% of Antarctic SO_4^{2-} comes from degassing volcanoes [*Cosme et al.*, 2005]. We recognize that estimation of the volcanic contribution is complex, because As/S values in published records vary largely. The volcanic contributions based on As/S ratios from different studies are shown in Figure 4.3. The highest As/S values are reported from Mount Erebus, an active volcano located in East Antarctica, that potentially could be a source of impurities at the South Pole and is suggested to have a regional impact over Antarctica [*Zreda-Gostynska et al.*, 1997]. Our calculations, using a maximum As/S concentration ratio value of 0.001364 from Mt Erebus [*Zreda-Gostynska et al.*, 1997], show that volcanic emission can contribute on average ~50% of the As budget at South Pole. The volcanic contribution is especially significant during periods of low As deposition at South Pole where it can account for ~ 80% of the total As. The volcanic contribution is relatively lower during periods of increased As concentrations (~20%) (Table 4.1), suggesting that during these times other sources are more important to the As budget.

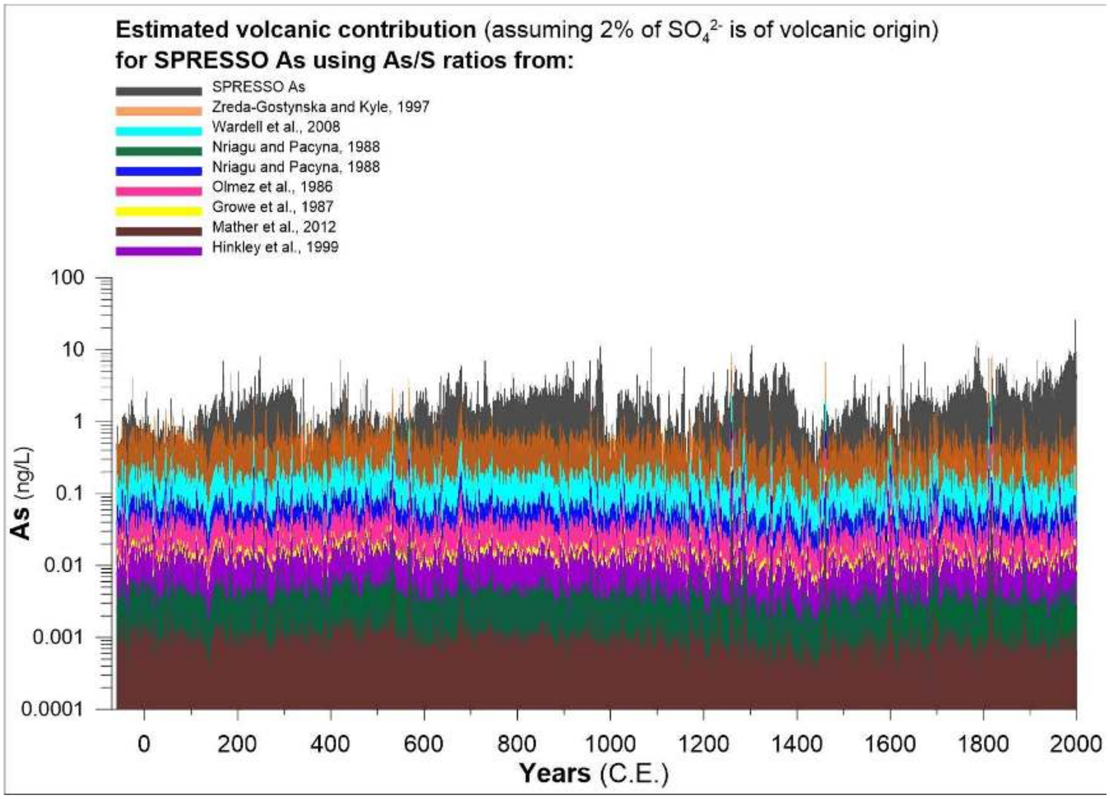

Figure 4.3 Estimated volcanic contribution for As using As/S values reported from volcanic plumes [*Olmez et al.*, 1986; *Crowe et al.*, 1987; *Nriagu and Pacyna*, 1988; *Zreda-Gostynska et al.*, 1997; *Hinkley et al.*, 1999; *Wardell et al.*, 2008; *Mather et al.*, 2012]

Another important natural source for As is biologically mediated marine and terrestrial volatilization [*Nriagu*, 1989; *Zhang et al.*, 2013]. Increases in organoarsenic compounds in surface waters have been associated with primary productivity as a result of methylation reactions by phytoplankton [*Zhang et al.*, 2013]. However, the lack of an As correlation ($r=-0.1$, $p<0.0001$) with non-sea-saltSO_4^{2-} ($nssSO_4^{2-}$) in our record (Figure 4.2), an indicator of marine biogenic productivity in Antarctica [*Cosme et al.*, 2005], suggests that marine biogenic input to South Pole As is not significant. Previous studies estimate that low temperature volatilization from soils could also contribute to the As budget [*Chilvers and Peterson*, 1987; *Nriagu*, 1989], however, published studies do not allow us to make any quantitative estimations of the terrestrial biogenic contribution for Antarctica. It is possible, though, that terrestrial biogenic emission could be important during periods of elevated As concentration.

We estimate that during periods of low As concentration a significant component comes from volcanic emissions and a relatively small fraction from soil dust (Table 4.1). Periods of low As concentrations usually correspond to intervals with decreased dust (Ti, La, Ce, Pr) and sea salt (Na) concentrations (Fig. 4.2). A decrease in dust elements and Na is interpreted as weaker atmospheric circulation, and therefore a decrease in As transport from more distant sources at these times, leaving the As budget at these times likely dominated by a local volcanic source such as Mt. Erebus.

During periods with high As deposition (Table 4.1), the volcanic source is relatively less significant suggesting that As is supplied to South Pole from other sources. Intervals with increased As concentration typically coincide with an increase in Na and dust elements (Ti, La, Ce, Pr) (Fig. 4.2) indicating enhanced aerosol loading of air entering South Pole. At these times it is likely that enhanced atmospheric circulation results in the transport of As from more distant sources, possibly bringing biogenic As from Southern Hemisphere land-masses. Intensified atmospheric circulation could, therefore, also transport anthropogenic source As from Southern Hemisphere countries.

4.4.3 Anthropogenic emissions.

Arsenic can enter the atmosphere from anthropogenic activities such as: non-ferrous metal smelting and mining, fossil fuel combustion, pesticides, herbicides, wood preservatives, burning of pasture land, and glass manufacture [*Chilvers and Peterson*, 1987; *Matschullat*, 2000; *Garelick et al.*, 2008]. Non-ferrous metal production, especially copper smelting, is the most significant source for As and is estimated to account for ~70% of worldwide anthropogenic As in the late

1990s [*Pacyna*, 1987]. Copper and copper alloys ores have been smelted in South America for more than 3,000 years [*Cooke et al.*, 2008b; *Cortés and Scattolin*, 2017] and we suggest that these metallurgical activities could have contaminated the atmosphere as far away as Antarctica with As.

Figure 4.2 shows several intervals with elevated As concentrations, that we suggest based on the foregoing, could be related to human activities. Increase in As concentrations between 225-325 CE could be caused by metallurgical activities of the Moche civilization in northern Peru [*Hörz and Kallfass*, 2000; *Eichler et al.*, 2017]. At the same time we observe an increase in dust concentrations indicating enhanced atmospheric circulation, thus As from more distant sources, such as northern Peru, could be transported to the South Pole site.

An increase in As concentrations between ~645-985 CE coincides with a period of active arsenic bronze metallurgy by the Wari and Tiwanaku empires in southern South America [*Cooke et al.*, 2008a]. Decreases in As concentrations around 985 CE coincide with the collapse of both empires (~1000 CE), suggesting that ancient native American metallurgical activity in South America potentially affected As deposition at the South Pole.

The next period of elevated As concentration (Figure 4.2) starting ~1260 CE, corresponds to the rise of the Inca civilization. However, As concentrations decline ~1400 CE and remain low from 1400 to ~1725 CE, despite an active Inca Empire and following widespread early Colonial metallurgy. Lower levels of As concentrations might be explained by two factors: a shift to weaker atmospheric transport to South Pole, as evidenced by relatively lower dust loading during this period (Figure 4.2); and a decrease in copper smelting and intensification of silver metallurgy during Colonial times.

Increased As concentration between ~1250-1400 CE also coincide with a period of rapid deforestation and associated burning in New Zealand following the Maori arrival [*McWethy et al.*, 2009]. High severity fires during the “Initial Burning Period” resulted in a rapid loss of nearly half of the native forest. Such a large burning event would release trace elements into the atmosphere and it is possible that increased As concentrations at South Pole at this time are related to the New Zealand forest fires.

Increases in As concentration since ~1730 correspond to the beginning of the industrial revolution. Numerous copper, gold and silver mines were opened in Chile during the 1700’s, and the copper industry continued to expand during the 18th and 19th centuries [*Conrad J. Bahre*, 1979]. Decrease in As between ~1800-1830 CE is believed to be related to stagnation of the mining industry during the South American War of Independence, after which As increased significantly during the period ~1830-1850 CE This time interval coincides with the introduction of fuel-fired reverberatory furnaces for copper smelting in Chile and the subsequent increase in smelting activities [*Conrad J. Bahre*, 1979]. At the same time (~1840 CE) southern Australia experienced a mining boom following the discovery of silver-lead and copper ores [*Australian Mining History Association*, 2011], which could also contribute to South Pole As enrichment.

4.4.4 Recent increase.

The most striking feature in the South Pole record is the As rise since 1975 CE As concentration increases 4.2 times, reaching a maximum in concentration of 26.15 ng/L, the highest value during the ~2000-year long record (Table 4.1, Figure 4.2). Dust elements and Na concentrations decrease during this time (Figure 4.2), indicating that the As increase is not related to the intensification of atmospheric circulation. Volcanic, sea salt and soil dust sources only account for ~3% of the total As at this time, indicating that the As is anthropogenic in origin.

Previous studies show that air traffic and activities at research stations can contaminate the local Antarctic environment near these stations [*Wolff and Cachier*, 1998; *Mazzera et al.*, 2001; *Korotkikh et al.*, 2014] However, elevated levels of As in recent decades are evident in several other Antarctic records located far from stations (Figure 4.4), demonstrating that the South Pole ice core As increase is not solely related to local station contamination, but is more likely caused by hemispheric scale input integrated from different sources. As mentioned above, Cu smelting is the biggest source of anthropogenic As [*Nriagu and Pacyna*, 1988; *Pacyna and Pacyna*, 2001]. Global modeling studies suggest that during the period 1999-2000 CE emissions from South America contributed up to 90% of the As deposition in Antarctica [*Wai et al.*, 2016].

Chile is the largest Cu producer in the world with an increasing trend in production since the early 19th century and a rapid rise since the 1970s [*British Geological Survey*, 2015] (Figure 3). We observe a significant correlation ($r=0.83$, $p<0.0001$) between As concentrations in the South Pole record and Chilean copper production. This correlation suggests that Cu smelting in Chile is a likely cause of the As enrichment in the South Pole ice core record. We note a decrease in As concentration in early 1998 CE, when As levels drop to an average of ~3.8 ng/L. The As level is still higher than during the pre-industrial period, however, it is significantly lower compared to 1970-1997 CE values. Other Antarctic records also show a decrease in As concentrations in the late 1990s (Figure 4.4). This decrease is coincident with the introduction of environmental regulations for airborne As emissions in Chile in 1990s.

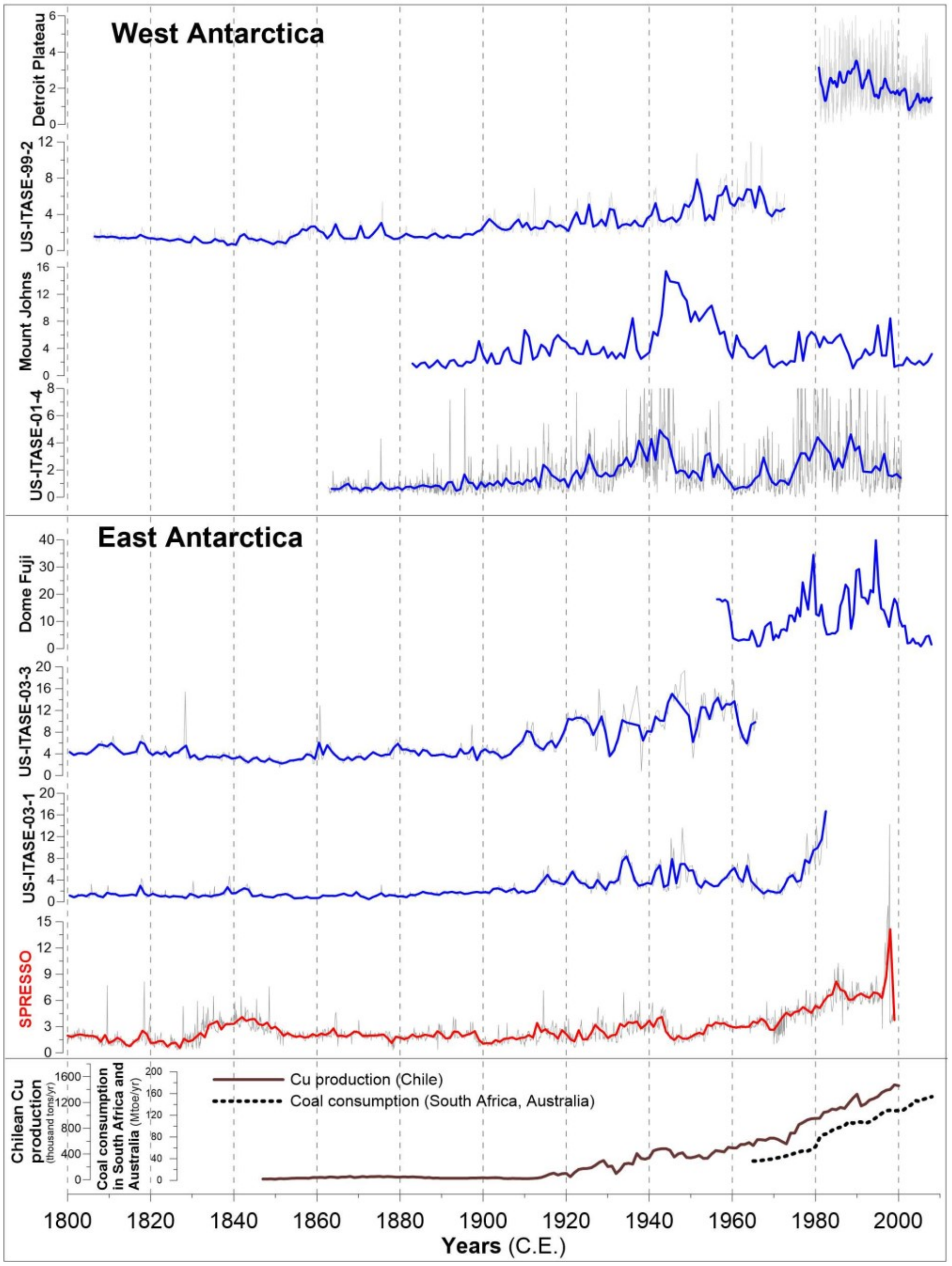

Figure 4.4 Comparison of South Pole As concentrations with other Antarctic ice core records. As records from the following sites are shown: Detroit Plateau [*Potocki et al.*, 2016], US-ITASE-99-2 [*Mayewski and Dixon*, 2013], US-Mount Jones [*Schwanck et al.*, 2016], ITASE-01-4 [*Mayewski and Dixon*, 2013], Dome Fuji [*Hong et al.*, 2012], US-ITASE-03-3 [*Mayewski and Dixon*, 2013], US-ITASE-03-1 [*Mayewski and Dixon*, 2013], and SPRESSO As concentrations (ng/L). The grey color lines show raw As data. The colored lines represent background levels estimated using a robust spline smoothing function. Chilean copper smelter production [*BritishGeologicalSurvey*, 2015], and Australian and South African coal consumption [*BP Statistical Review of World Energy*, 2015] are also shown.

The first set of regulations were established in 1991, and further regulation was passed in 1999 [*Caldentey and Mondschein*, 2003]. The decline in As concentrations at the South Pole and other Antarctic records suggests that environmental regulations in Chile and consequent reduction of As emission from Cu smelters [*Caldentey and Mondschein*, 2003] have resulted in some success.

The second to largest anthropogenic source for atmospheric As after Cu smelting is coal combustion, which can account for up to 22% of anthropogenic As [*Nriagu and Pacyna*, 1988; *Pacyna and Pacyna*, 2001]. The consumption of fossil fuels in Southern Hemisphere countries has continuously increased during recent decades. South Africa, the biggest coal consumer in the Southern Hemisphere, burned ~1930 million tonnes of oil equivalent (Mtoe) of coal during 1965-2000 CE, followed by Australia, which consumed ~950 Mtoe [*BP Statistical Review of World Energy*, 2015]. We found high positive correlations between South Pole As concentrations and coal consumption in South Africa of $r=0.6$ ($p<0.0001$) and As and coal consumption in Australia of $r=0.7$ ($p<0.0001$) (Figure 4.4). This indicates that coal consumption is at least partially responsible for the enrichment in As at the South Pole during recent decades.

4.4.5 Differences between East and West Antarctic As deposition.

Comparison of Antarctic As ice core records is difficult, since some of the records do not cover the period since 1975 CE or only show limited time intervals. Figure 4.4 reveals a difference between East and West Antarctic As records (Figure 4.5). East Antarctic records show a rapid increase in As concentration since ~1975 CE West Antarctic As records show a different pattern with two periods of elevated As concentrations: ~1935-1960 CE and ~1975-1999 CE

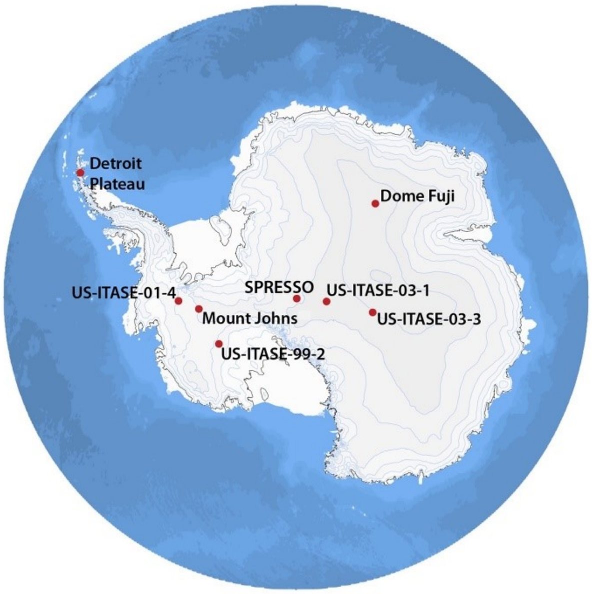

Figure 4.5 Map of Antarctica showing locations of ice core sites used in this study. Map produced using Generic Mapping Tools (GMT) [*Wessel et al.*, 2013], http://gmt.soest.hawaii.edu/, version 4.5.12.

The increase during the most recent period is not as significant as in the East Antarctic ice core records. While East Antarctic As records show a similar increasing trend to Chilean copper production, West Antarctic As concentrations do not reveal this association. The difference between As trends could be due to the different atmospheric circulation patterns impacting these regions. West Antarctica is strongly influenced by lower atmospheric transport, enhanced by cyclonic activity. More elevated inland East Antarctic sites are more influenced by mid and upper-troposphere air masses [*Sudarchikova et al.*, 2015].

A major low pressure system in the area of the Amundsen/Ross Seas, the Amundsen Sea Low (ASL), has a significant effect on climatic conditions in West Antarctica [*Raphael et al.*, 2016]. The strength and position of the ASL is influenced by the phase of the Southern Annual Mode (SAM), a primary mode that controls extratropical Southern Hemisphere climate variability. Since the late 1950s, the SAM has been shifting to a more positive mode, with the major shift occurring in the mid-1970s [*Thompson and Wallace*, 2000; *Marshall*, 2003a]. The shift to a positive SAM has resulted in an intensification of westerly flow around Antarctica and the contraction of the polar vortex [*Mayewski et al.*, 2013]. While intensification of the westerlies leads to more efficient poleward transport to East Antarctica, it might have the opposite effect on West Antarctic sites. Stronger westerly flow has caused the ASL to move eastward closer to the Antarctic Peninsula [*Cullather et al.*, 1996; *Turner et al.*, 2013]. When the ASL is located further eastward, one consequence is low net precipitation in West Antarctica [*Kreutz et al.*, 2000]. This might explain the lack of increase in As concentrations in West Antarctic sites since 1975 CE Another factor that could affect As deposition in Antarctica is the different dominant dust sources. Previous studies show that South American sources dominate dust deposition in East Antarctica, and that Australia is a more important source for West Antarctica [*Li et al.*, 2008; *Albani et al.*, 2012]. Thus, As emitted from copper smelting activities in Chile is more efficiently transported by westerly flow to downwind East Antarctic sites.

4.5. Summary.

This study presents a high-resolution record of As variability for the period from 60 BCE to 1999 CE The South Pole As record shows high variability with several periods of increased concentrations. Most of the As is attributed to volcanic emissions from Mount Erebus during periods of low As deposition. Intervals with increased As concentrations are most likely related to increased anthropogenic emissions in the Southern Hemisphere countries and partially to the intensification of atmospheric transport. Our record suggests that anthropogenic activities in the Southern Hemisphere might have contaminated the natural As budget during the last two millennia: notably during 645-985 CE due to the mining and smelting activities by Wari and Tiwanaku empires and during 1260-1400 CE due to activities carried out by the Incas and possibly

Maori. Elevated As concentrations since ~1730 CE are most likely related to anthropogenic activities in South America and Australia. The most significant increase in As occurs after 1975 CE and is attributed to increased copper smelting in Chile and partially to coal combustion in the Southern Hemisphere. A similar rise is observed in other East Antarctic sites, but not in West Antarctica. This differences in As deposition is attributed to the different atmospheric pathways and changes in atmospheric circulation since the mid-1970s. More specifically, the southward shift in the polar vortex since the 1970s and the consequent increase in the strength of the westerlies.

CHAPTER 5

RECENT INCREASE IN BARIUM CONCENTRATIONS AS RECORDED IN A SOUTH POLE ICE CORE

5.1 Abstract

Here we present high-resolution (~9.4 samples/year) records of Ba concentrations for the period from 1541 to 1999 CE obtained from an ice core recovered at the South Pole (US ITASE-02-6) site. We note a significant increase in Ba concentration (by a factor of ~23) since 1980 CE The Ba crustal enrichment factor (EFc) values rise from ~3 before 1980 CE to ~32 after 1980 CE. None of the other measured major and trace elements reveal such significant increases in concentrations and EFc values. Comparison with previously reported Antarctic Ba records suggests that significant increases in Ba concentrations at South Pole since 1980 CE are most likely caused by local source pollution. The core was collected in close proximity to Amundsen-Scott South Pole Station; therefore activities at the station, such as diesel fuel burning and intense aircraft activity, most likely caused the observed increase in Ba concentrations and its EFc values in the South Pole ice core record.

5.2. Introduction

Human activities now have a major impact on the global atmospheric cycles of many trace elements. A number of studies show that even the remote Antarctic continent is significantly contaminated by heavy metals due to anthropogenic activities in the Southern Hemisphere. Several Antarctic records show clear evidence of anthropogenic influence on the Pb cycle in the Antarctic [*Barbante et al.*, 1997; *Planchon et al.*, 2002a; *Vallelonga et al.*, 2002; *Hur et al.*, 2007] Increased concentrations of Cu, Cr, Zn, Ag, Pb, and Bi have been observed during recent decades [*Wolff and Cachier*, 1998; *Wolff et al.*, 1999; *Planchon et al.*, 2002a; *Hur et al.*, 2007] and the elevated values of these metals in Antarctica are attributed to atmospheric emissions from human activities in South America, Southern Africa and Australia [*Planchon et al.*, 2002a].

Activities at research stations, tourist ships and air traffic, are also contributing to contamination over the Antarctic environment. Model simulations by [*Graf et al.*, 2010] show that ship emissions, both sulfurous and black carbon, dominate anthropogenic pollution near the Antarctic coast. Another study conducted at Halley Research station links black carbon contamination with emissions from station generators [*Wolff and Cachier*, 1998]. Higher concentrations of carbon particles, Pb and Zn are reported near McMurdo Station likely due to station activities [*Mazzera et al.*, 2001].

Here we present a ~450-year record of atmospheric Ba concentrations as recorded in a South Pole ice core. Several previous studies have reported records of Ba concentrations in Antarctica [*Planchon et al.*, 2002a; *Van de Velde et al.*, 2005; *Hur et al.*, 2007; *Dixon et al.*, 2012; *Hong et al.*, 2012]. They show that rock and soil dust is a major source for Ba in Antarctica and several studies use Ba concentrations in snow and ice samples as a proxy for natural source dust input to evaluate potential anthropogenic contributions for other elements [*Van de Velde et al.*, 2005; *Burn-Nunes et al.*, 2011; *Hong et al.*, 2012]. Our records indicate that Ba in Antarctica itself is affected by local source pollution.

5.3. Methodology

Detailed description about core collection and processing, sample analysis, and timescale development are in Chapter 2. This study is focused on changes in Ba concentration in the South Pole ice core chemistry record. Detection limit for Ba (defined as three times the standard deviation of MilliQ (>18.2 MΩ) deonized water blanks passed through the entire melter system) is 0.31 ng/L, equivalent to ~1.1% of the Ba mean concentration over the analyzed period (Table 2.1).

Locations of the South Pole US ITASE-02-6 and other ice core sites used in this study are shown in Figure 5.1.

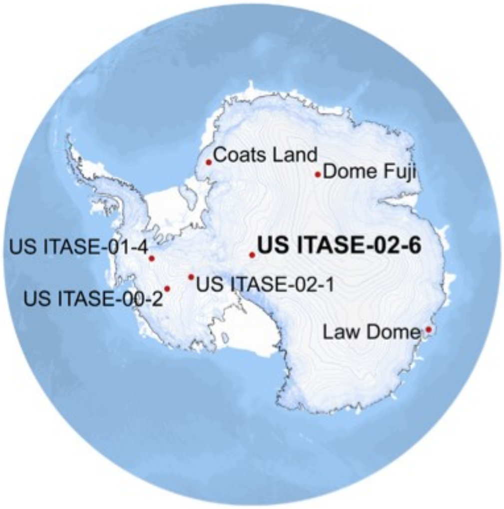

Figure 5.1 Location of the US ITASE-02-6, 02-1, 00-2 and 01-4 ice core drilling sites in Antarctica. Also shown are locations of the Dome Fuji (Hong et al., 2012), Coats Land (Planchon et al., 2002), and Law Dome (Vallelonga et al., 2002) snow pit sampling and firn/ice core drilling sites.

5.4 Results

5.4.1 Variations in elemental concentrations for the period 1541-1999 CE

Figure 5.2 shows variations in Ba concentration from the South Pole ice core for the period from 1541 to 1999 CE Concentrations vary from 0.01 to ~3000 ng/L, with a mean concentration during the entire period of ~28.3 ng/L. Low background concentrations of Ba (average of ~12.9 ng/L) are observed between 1541 and 1980 CE (Figure 5.2, Table 5.1). During this period maximum Ba concentration is 252.8 ng/L. Since 1980 CE Ba concentrations increase significantly by a factor of ~23, reaching a mean value of ~296 ng/L, varying from a minimum value of 5.2 ng/L up to a maximum value of 3118 ng/L. No other measured elements have such a significant increase since 1980 CE

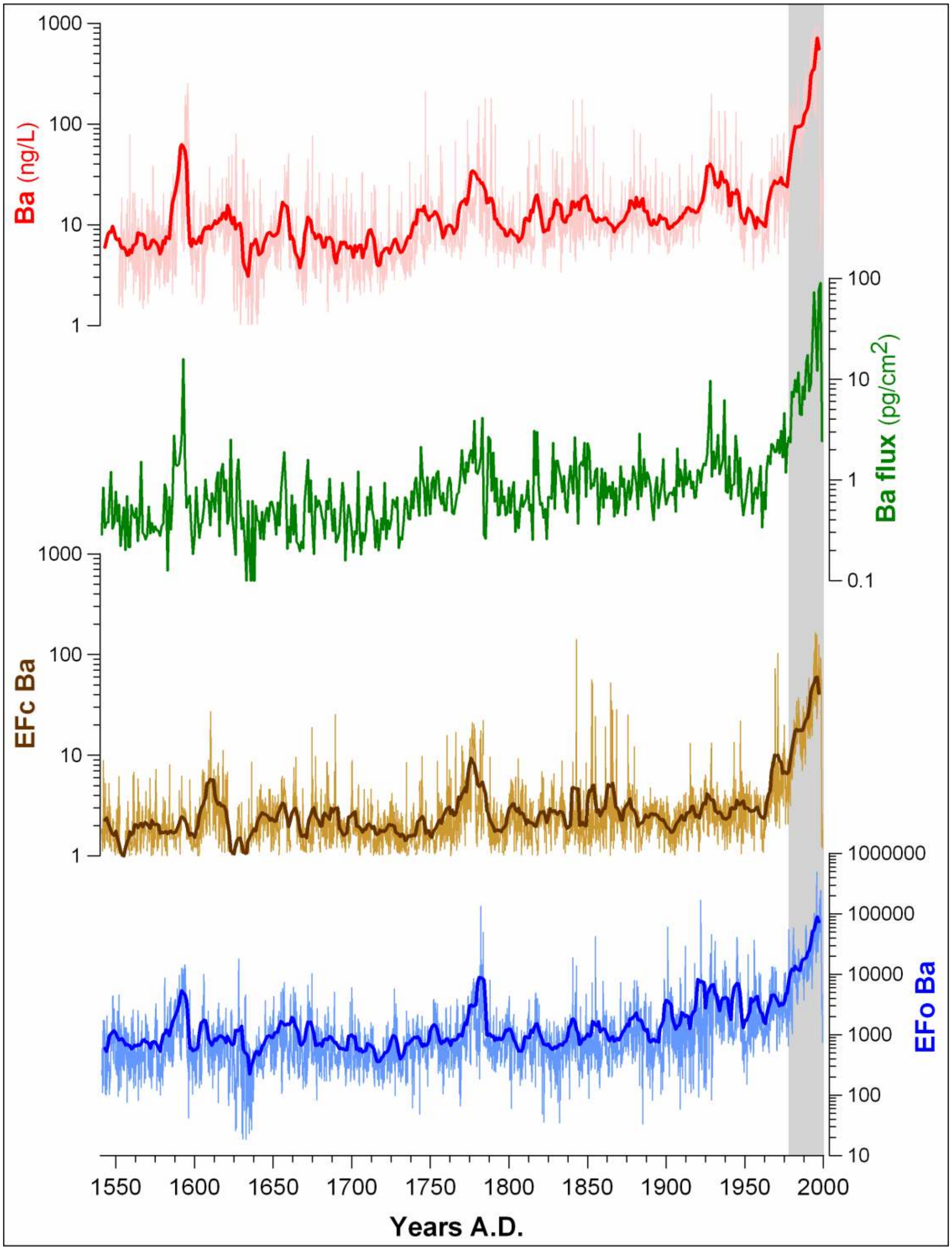

Figure 5.2 South Pole Ba concentration (ng/L), Ba flux, and enrichment factor values for the period 1541 to 1999 CE. The light color lines in concentration, EFc and EFo profiles are raw data and the dark color lines are the 5-year running mean. The shaded area represents the period of increased Ba concentration, flux and EF values.

5.4.2 Concentration versus Flux

To investigate if observed changes in chemistry are related to changes in accumulation rate, we calculate Ba annual deposition flux. Ba flux is calculated by multiplying Ba concentrations in the ice by the annual water-equivalent accumulation rate (weq=density x annual layer thickness). Figure 5.2 shows Ba concentration and flux for the period 1541-1999 CE Both concentration and flux show similar variability and increase in the late 20th century. This indicates that the South Pole Ba concentrations are independent of accumulation rate and that the variability exhibited in the record is likely not a function of changes in snow accumulation.

5.4.3 Crustal Enrichment Factor

Atmospheric dust is one of the major sources for trace elements in ice cores. Ba has been used as a proxy for crustal dust input to Antarctica in several studies [*Vallelonga et al.*, 2002; *Van de Velde et al.*, 2005; *Hong et al.*, 2012]. To investigate the importance of crustal dust attribution for Ba in the South Pole ice core, we calculate a mean crustal Enrichment Factor (EFc) for Ba using the following equation:

$$EFc = \left[\frac{\left({}^{Ba}\!/\!_{La} \right)_{sample}}{\left({}^{Ba}\!/\!_{La} \right)_{UCC}} + \frac{\left({}^{Ba}\!/\!_{Ce} \right)_{sample}}{\left({}^{Ba}\!/\!_{Ce} \right)_{UCC}} + \frac{\left({}^{Ba}\!/\!_{\mathrm{Pr}} \right)_{sample}}{\left({}^{Ba}\!/\!_{\mathrm{Pr}} \right)_{UCC}} + \frac{\left({}^{Ba}\!/\!_{Ti} \right)_{sample}}{\left({}^{Ba}\!/\!_{Ti} \right)_{UCC}} \right] \Bigg/ 4$$

Upper continental crust (UCC) values of La, Ce, Pr, and Ti are from Wedepohl [*Wedepohl*, 1995]. We calculate a mean EFc using four reference elements to reduce the potential bias from any one crustal reference element. The four crustal reference elements (La, Ce, Pr, and Ti) were chosen because their EFc ratios to one another in the South Pole ice core are close to ~1 (Figure 5.3). Therefore, they are a good proxy for crustal dust for this study.

Figure 5.3 shows Ba EFc values for the study period. Usually, elements with EFc lower than 10 are considered non-enriched and as such are considered delivered almost entirely from crustal dust [*Duce*, 1975]. Variations of EFc in elements between 0 and 10 are attributed to the differences in the composition of crustal dust reaching the study site [*Tuncel et al.*, 1989; *Siggaard-Andersen et al.*, 2007]. Our calculations show that for the period from 1541 to ~1980 CE, Ba EFc values are very low (mean of 2.8) (Table 5.1). This indicates that the major source for the Ba during this time is crustal dust. Since 1980 CE Ba EFc values increase significantly to a median value of 32.1 indicating that other sources besides crustal dust were introduced during recent decades. Therefore, the recent increase in Ba concentration is not related to an increase of crustal dust input to Antarctica.

5.4.4 Oceanic Enrichment Factor

To evaluate possible contributions to Ba concentrations from marine aerosols we calculated a Ba oceanic enrichment factor (EFo). EFo values for Ba were calculated according to the following equation:

$$EFo = \frac{\left(Ba/Na\right)_{sample}}{\left(Ba/Na\right)_{ocean\ water}}$$

Ocean elemental abundances are from Lide [*Lide*, 2005]. Figure 5.3 shows that Ba is highly enriched relative to ocean water over the entire record, indicating that the marine contribution for Ba at South Pole is negligible and is not the cause of the Ba rise since 1980 CE

Both EFc and EFo calculations suggest that during the period from 1541 to ~1980 CE most of the Ba originated from rock and soil dust, however since 1980 CE another source, most likely anthropogenic emissions, became more significant.

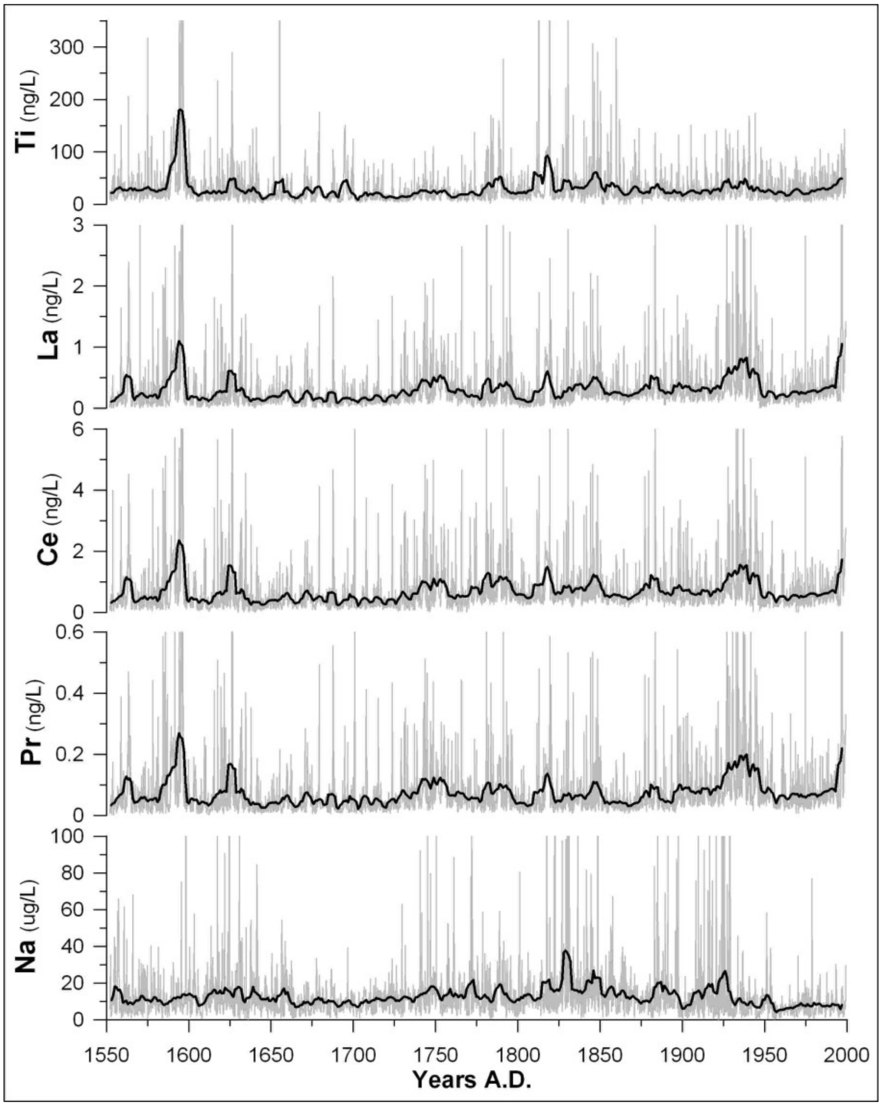

Figure 5.3 South Pole concentration of Ti (ng/L), La (ng/L), Ce (ng/L), Pr (ng/L) and Na (ug/L) for the period 1541 to 1999 CE. The light color lines are raw data and the dark color lines are the 5-year running mean.

5.5. Discussion and conclusion

In order to determine whether the post 1980 CE Ba increase is local, or if it represents a higher Ba loading (eg., increased atmospheric transport) to the entire Antarctic continent, we compared Ba concentrations in the South Pole ice core with other available Antarctic glaciochemical Ba records (Figures 5.1, 5.4, Table 5.1). Table 1 shows that all sites have mean Ba concentration values similar in magnitude to pre-1980 CE South Pole values both before and after

1980 CE Law Dome has the lowest Ba concentration, what could be explained by higher snow accumulation at this site.

Table 5.1 Average concentrations of Ba and average crustal enrichment factor (EFc) values in Antarctic ice core records.

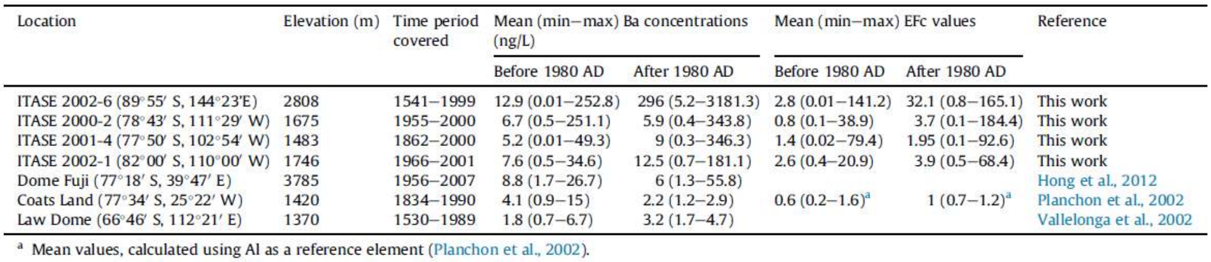

Location	Elevation (m)	Time period covered	Mean (min–max) Ba concentrations (ng/L)		Mean (min–max) EFc values		Reference
			Before 1980 AD	After 1980 AD	Before 1980 AD	After 1980 AD	
ITASE 2002-6 (89°55′ S, 144°23′E)	2808	1541–1999	12.9 (0.01–252.8)	296 (5.2–3181.3)	2.8 (0.01–141.2)	32.1 (0.8–165.1)	This work
ITASE 2000-2 (78°43′ S, 111°29′ W)	1675	1955–2000	6.7 (0.5–251.1)	5.9 (0.4–343.8)	0.8 (0.1–38.9)	3.7 (0.1–184.4)	This work
ITASE 2001-4 (77°50′ S, 102°54′ W)	1483	1862–2000	5.2 (0.01–49.3)	9 (0.3–346.3)	1.4 (0.02–79.4)	1.95 (0.1–92.6)	This work
ITASE 2002-1 (82°00′ S, 110°00′ W)	1746	1966–2001	7.6 (0.5–34.6)	12.5 (0.7–181.1)	2.6 (0.4–20.9)	3.9 (0.5–68.4)	This work
Dome Fuji (77°18′ S, 39°47′ E)	3785	1956–2007	8.8 (1.7–26.7)	6 (1.3–55.8)			Hong et al., 2012
Coats Land (77°34′ S, 25°22′ W)	1420	1834–1990	4.1 (0.9–15)	2.2 (1.2–2.9)	0.6 (0.2–1.6)[a]	1 (0.7–1.2)[a]	Planchon et al., 2002
Law Dome (66°46′ S, 112°21′ E)	1370	1530–1989	1.8 (0.7–6.7)	3.2 (1.7–4.7)			Vallelonga et al., 2002

[a] Mean values, calculated using Al as a reference element (Planchon et al., 2002).

The South Pole average concentration for the whole analyzed period is 28.3 ng/L and is relatively stable during the entire record except for recent decades. Since ~1980 CE Ba concentrations in the South Pole ice core increase dramatically, reaching a mean value of 296 ng/L. Other glaciochemical records that cover recent decades, such as US ITASE-00-2, US ITASE-01-4, US ITASE-02-1, Dome Fuji [*Hong et al.*, 2012], Coats Land [*Planchon et al.*, 2002a] and Law Dome [*Vallelonga et al.*, 2002], do not demonstrate a notable rise since 1980 CE (Figure 5.4). Therefore it is most likely that the increase in Ba concentrations at South Pole since 1980 CE can be attributed to a local source.

We also calculate Ba EFc values for the other sites. Ba EFc values for other US ITASE ice core records were calculated using the same method as described in section 5.3. We were not able to do the same EFc calculations for the Dome Fuji, Law Dome and Coats Land records, since they did not have companion measurements for La, Ce, Pr and Ti (crustal reference elements used in this study). For Coats Land we used previously published Ba EFc values based on a calculation using Al as a reference element [*Planchon et al.*, 2002a]. Calculated Ba EFc values are shown in Table 5.1 and Figure 5.5. Other US ITASE (US ITASE-01-4, 02-1, and 03-1) and Coats Land records have mean Ba EFc values below 10 both before and after 1980 CE, indicating that crustal dust is the primary source for Ba in Antarctic ice. None of the other Antarctic records show increases in Ba EFc values since 1980 CE, as is evident in the South Pole record (Figure 5.5). This further suggests that an increase in Ba concentrations during recent decades at South Pole is most likely caused by local source pollution.

Anthropogenic release of Ba is primarily associated with industrial processes involved in the mining, refining, and production of Ba and barium-based chemicals, and fossil fuel combustion [*Miner*, 1969]. Since other Antarctic records do not demonstrate a rise in Ba concentrations we exclude any global or hemispheric-scale sources of Ba pollution, such as mining and production of Ba and barium-based chemicals. Barium in the form of organometallic compounds is also used as an additive to diesel fuels to reduce smoke emissions from diesel engines [*Miner*, 1969; *Schroeder*, 1970; *No and Patterson*, 1982]. The South Pole ice core was collected 5 kilometers from the Amundsen-Scott South Pole Station. This is an active station that requires a large amount of diesel fuel to power and heat it. Thus, anthropogenic activities at Amundsen-Scott Station, such as diesel fuel combustion and intensive aircraft activity are likely to be responsible for the increased Ba concentrations observed in the South Pole ice core in recent decades.

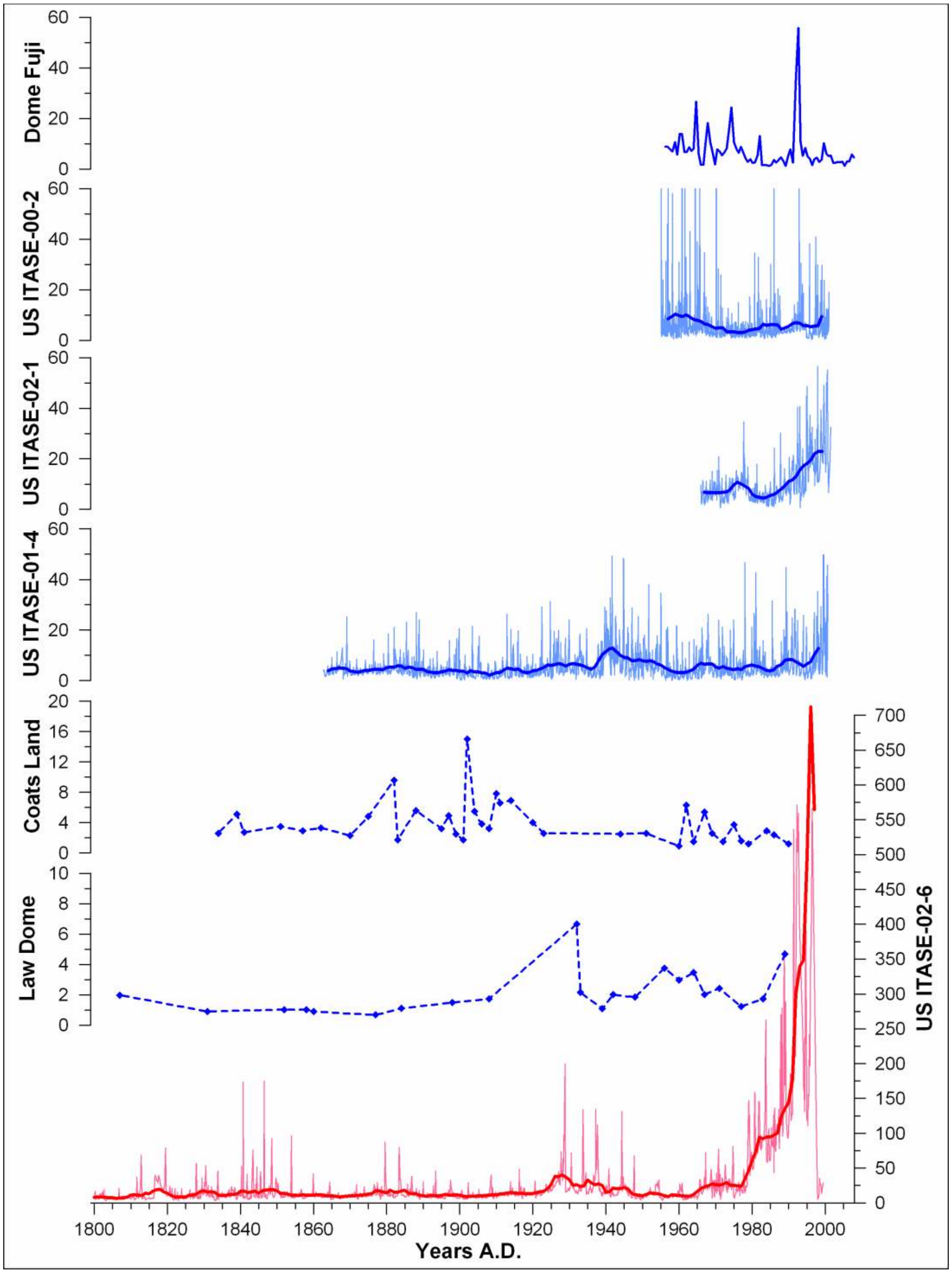

Figure 5.4 Comparison of Ba records from different Antarctic sites for the period from 1800 CE to 2002 CE. Ba concentration profiles from the South Pole US ITASE-02-6, 02-1, 00-2 and 01-4 ice core drilling sites (this study); Dome Fuji (Hong et al., 2012), Coats Land (Planchon et al., 2002) and Law Dome (Vallelonga et al., 2002). All concentrations are in ng/L. The light color lines in Ba records from ITASE sites are raw data and the dark color lines are mean background level (estimated using 5-year running mean).

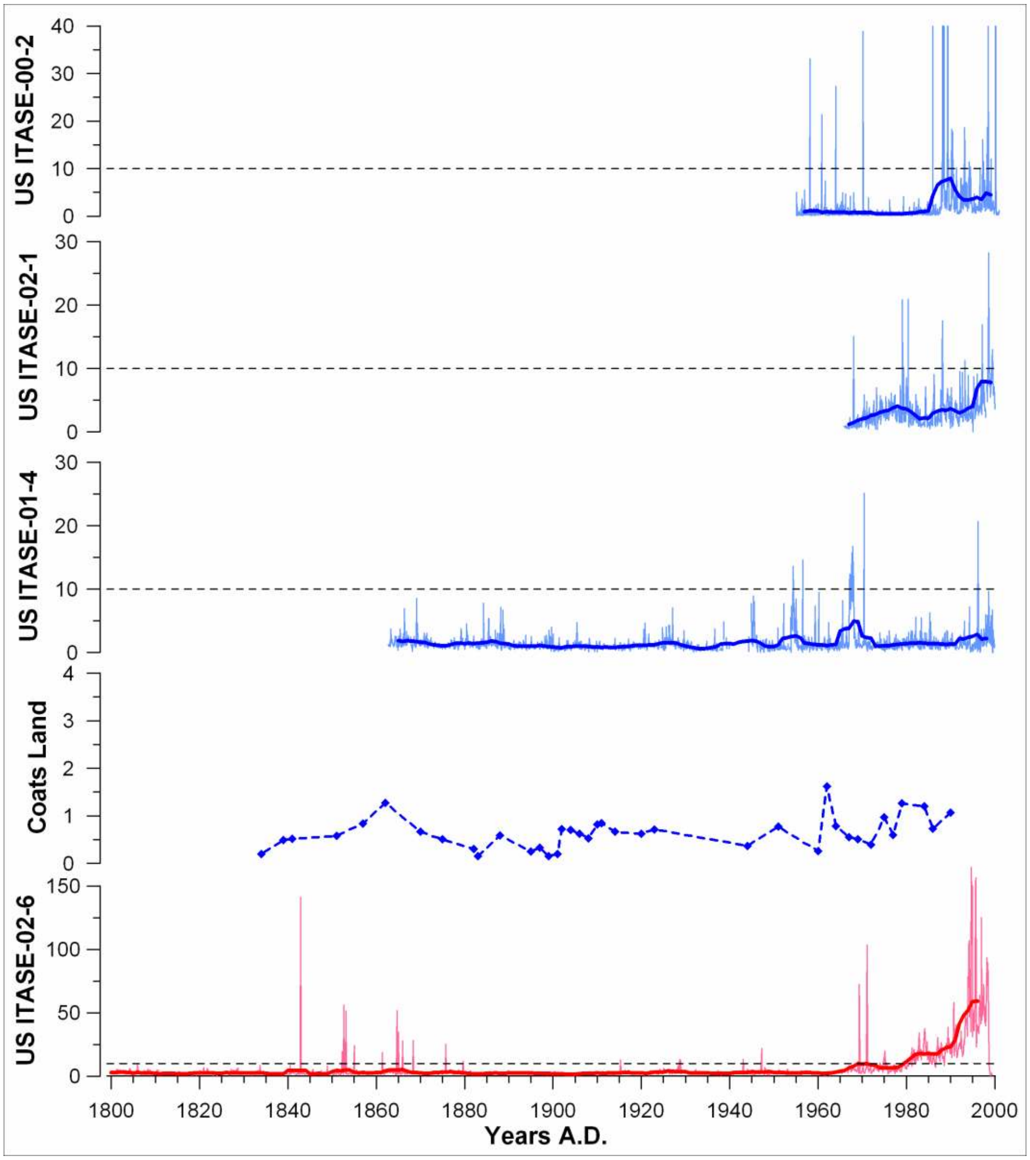

Figure 5.5 Estimated Ba EFc profiles from the Antarctic ice cores. Data shown from the US ITASE-02-6 (South Pole), 02-1, 00-2 and 01-4 ice core drilling sites (this study) and from Coats Land (Planchon et al., 2002). The light color lines in Ba EFc records are raw data and the dark color lines are mean background level (estimated using 5-year running mean).

CONCLUSION

6.1. Chapter 3 Summary

This study presents an ~2000 year-long high-resolution records of SO_4^{2-}, NO_3^-, Ti, La, Ce, Pr, $\delta^{18}O$, δD, d-excess, and accumulation from the South Pole. Our record reveals major changes in SO_4^{2-}, dust, NO_3^-, stable water isotopes, and accumulation rate during the period between 1400-1700 CE. Together the South Pole records demonstrate a major reorganization of atmospheric circulation between ~1400-1700 CE, corresponding to the initial stages of the Little Ice Age (LIA). The South Pole records show that the atmospheric reorganization at the onset of the LIA occurred in two major steps. The first shift ~1400 CE is evident by a decline in dust and SO_4^{2-} concentrations. We suggest that ~1400 CE SHWs started to intensify and move south, shifting away from sources of dust and SO_4^{2-} in the midlatitudes. The decrease in SO_4^{2-} during the LIA possibly indicates a decrease in sea ice extent in the Weddell Sea. Increase in stable water isotope values, decrease in d-excess, and NO_3^- concentration defines the second shift in atmospheric circulation ~1650-1700 CE. Changes in the South Pole time series since ~1650 CE indicate increased cyclonic activity and subsequent enhanced penetration of marine air masses to the South Pole, displacement of the moisture source to a colder higher latitude ocean location, reduction of the katabatic air transport to the South Pole from the interior of East Antarctica, and a more pronounced contraction and intensification of the SHWs.

6.2. Chapter 4 Summary

This study presents a high-resolution record of As variability for the period from 60 BCE to 1999 CE. Our South Pole As record exhibits several periods of increased concentration: ~225-325 CE, ~645-985 CE, ~1260-1400 CE, and ~1730-1999 CE. The most significant increase in As concentration is observed after 1975 CE, when concentrations average 6.6 ng/L, which is four times higher than during the period before 1974 CE.

Estimation of the natural contribution to the As budget shows that emission from quiescently degassing volcanoes is the primary natural source for As. It is possible that terrestrial biogenic emission could also be an important source for the As at the South Pole. The most significant anthropogenic source for As is a copper smelting. Copper and copper alloys ores have been smelted in South America for more than 3,000 years [*Cooke et al.*, 2008b; *Cortés and Scattolin*, 2017] and periods of elevated As values coincide with periods of ancient active metallurgy. We suggest that these metallurgical activities could have contaminated the atmosphere with As as far away as Antarctica during the last 2000 years.

The most significant increase in As is observed since 1975 CE and is attributed to increased copper smelting in Chile and partially to coal combustion in the Southern Hemisphere. The other Antarctic ice core records also show increases in As during recent decades, however, the magnitude varies at different locations. Differences in As deposition are attributed to differing atmospheric pathways and changes in atmospheric circulation since the mid-1970s, such as the southward shift in the polar vortex since and the consequent increase in the strength of the SHWs.

6.3. Chapter 5 Summary

Ba concentrations have been measured in the South Pole ice core for the last ~500 years. The most significant increase in Ba (by a factor of ~23) is observed since 1980 CE. Calculation of crustal enrichment factor values shows that prior to 1980 CE the major source for Ba is crustal dust. The increased enrichment factor after 1980 indicates possible anthropogenic input. Comparison with Ba records from other Antarctic ice core sites shows that a significant increase in Ba concentration is only evident in the South Pole record. Since South Pole ice core was collected 5 km away from the Amundsen-Scott station, we suggest that the increase in Ba since 1980 CE is caused by pollution from the activities at the station, such as diesel fuel combustion and intensive aircraft activity.

REFERENCES

Abram, N. J., R. Mulvaney, F. Vimeux, S. J. Phipps, J. Turner, and M. H. England (2014), Evolution of the Southern Annular Mode during the past millennium, *Nat. Clim. Chang.*, *4*(7), 564–569, doi:10.1038/nclimate2235.

Albani, S., N. M. Mahowald, B. Delmonte, V. Maggi, and G. Winckler (2012), Comparing modeled and observed changes in mineral dust transport and deposition to Antarctica between the Last Glacial Maximum and current climates, *Clim. Dyn.*, *38*(9–10), 1731–1755, doi:10.1007/s00382-011-1139-5.

Australian Mining History Association (2011), Hahndorf , South Australia, in *Australia's Earliest Mining Era Mount Lofty Ranges 1841-1851*, pp. 4–8.

Barbante, C., C. Turetta, G. Capodaglio, and G. Scarponi (1997), Recent Decrease in the Lead Concentration of Antarctic Snow, *Int. J. Environ. Anal. Chem.*, *68*(4), 457–477, doi:10.1080/03067319708030847.

Barbante, C. et al. (2006), One-to-one coupling of glacial climate variability in Greenland and Antarctica, *Nature*, *444*(7116), 195–198, doi:10.1038/nature05301.

Bertler, N. A. N., P. A. Mayewski, and L. Carter (2011), Cold conditions in Antarctica during the Little Ice Age - Implications for abrupt climate change mechanisms, *Earth Planet. Sci. Lett.*, *308*(1–2), 41–51, doi:10.1016/j.epsl.2011.05.021.

Bhattacharya, P., A. H. Welch, K. G. Stollenwerk, M. J. McLaughlin, J. Bundschuh, and G. Panaullah (2007), Arsenic in the environment: Biology and Chemistry, *Sci. Total Environ.*, *379*(2–3), 109–120, doi:10.1016/j.scitotenv.2007.02.037.

Bodhaine, B. B. A., J. J. Deluisi, J. M. Harris, and G. Monitoringfor (1986), Aerosol measurements at the South Pole, , (January 1977), 223–235, doi:10.1111/j.1600-0889.1986.tb00189.x.

BP Statistical Review of World Energy (2015), BP Statistical Review of World Energy, Available from: http://www.bp.com/en/global/corporate/energy-economics/statistical-review-of-world-energy.html

BritishGeologicalSurvey (2015), World Mineral Statistics, Available from: http://www.bgs.ac.uk/mineralsuk/statistics/worldArchive.html

Brook, E. J., J. W. C. White, A. S. M. Schilla, M. L. Bender, B. Barnett, J. P. Severinghaus, K. C. Taylor, R. B. Alley, and E. J. Steig (2005), Timing of millennial-scale climate change at Siple Dome, West Antarctica, during the last glacial period, *Quat. Sci. Rev.*, *24*(12–13), 1333–1343, doi:10.1016/j.quascirev.2005.02.002.

Burn-Nunes, L. J. et al. (2011), Seasonal variability in the input of lead, barium and indium to Law Dome, Antarctica, *Geochim. Cosmochim. Acta*, *75*(1), 1–20, doi:10.1016/j.gca.2010.09.037.

Caldentey, R., and S. Mondschein (2003), Policy Model for Pollution Control in the Copper Industry, Including a Model for the Sulfuric Acid Market, *Oper. Res.*, *51*(1), 1–16, doi:10.1287/opre.51.1.1.12797.

Carleton, A. M. (2003), Atmospheric teleconnections involving the Southern Ocean, *J. Geophys. Res.*, *108*(C4), 8080, doi:10.1029/2000JC000379.

Ceppi, P., Y. T. Hwang, X. Liu, D. M. W. Frierson, and D. L. Hartmann (2013), The relationship between the ITCZ and the Southern Hemispheric eddy-driven jet, *J. Geophys. Res. Atmos.*, *118*(11), 5136–5146, doi:10.1002/jgrd.50461.

Chambers, F. M., S. A. Brain, D. Mauquoy, J. McCarroll, and T. Daley (2014), The ‘Little Ice Age’ in the Southern Hemisphere in the context of the last 3000 years: Peat-based proxy-climate data from Tierra del Fuego, *Holocene*, *24*(12), 1649–1656, doi:10.1177/0959683614551232.

Chilvers, D., and P. Peterson (1987), Global cycling of arsenic, *Lead, Mercur. cadmium Arsen. Environ.*, 279–301.

Conrad J. Bahre (1979), Destruction of the Natural Vegetation of North-Central Chile, *Univ. Calif. Publ. Geogr.*, *23*.

Cooke, C. A., M. B. Abbott, and A. P. Wolfe (2008a), Late-Holocene atmospheric lead deposition in the Peruvian and Bolivian Andes, *The Holocene*, *18*(2), 353–359, doi:10.1177/0959683607085134.

Cooke, C. A., M. B. Abbott, and A. P. Wolfe (2008b), Metallurgy in Southern South America, *Encycl. Hist. Sci. Technol. Med. Non-Western Cult. Vol. 2*, (Lechtman 1976), 1658–1662.

Cortés, L. I., and M. C. Scattolin (2017), Ancient metalworking in South America: a 3000-year-old copper mask from the Argentinian Andes, *Antiquity*, *91*(357), 688–700, doi:10.15184/aqy.2017.28.

Cosme, E., F. Hourdin, C. Genthon, and P. Martinerie (2005), Origin of dimethylsulfide, non-sea-salt sulfate, and methanesulfonic acid in eastern Antarctica, *J. Geophys. Res. D Atmos.*, *110*(3), 1–17, doi:10.1029/2004JD004881.

Crowe, B. M., D. L. Finnegan, W. H. Zoller, and W. V. Boynton (1987), Trace element geochemistry of volcanic gases and particles from 1983–1984 eruptive episodes of Kilauea Volcano, *J. Geophys. Res.*, *92*(B13), 13708, doi:10.1029/JB092iB13p13708.

Cullather, R. I., D. H. Bromwich, and M. L. Van Woert (1996), Interannual variations in Antarctic precipitation related to El Niño-Southern Oscillation, *J. Geophys. Res.*, *101*, 19109, doi:10.1029/96JD01769.

Dixon, D. a., P. A. Mayewski, I. D. Goodwin, G. J. Marshall, R. Freeman, K. A. Maasch, and S. B. Sneed (2012), An ice-core proxy for northerly air mass incursions into West Antarctica, *Int. J. Climatol.*, *32*(10), 1455–1465, doi:10.1002/joc.2371.

Duce, R. A. et al. (1975), Atmospheric trace metals at remote northern and southern-hemisphere sites - pollution or natural?, *Science (80-.).*, *187*, 59–61.

Eichler, A., G. Gramlich, T. Kellerhals, L. Tobler, T. Rehren, and M. Schwikowski (2017), Ice-core evidence of earliest extensive copper metallurgy in the Andes 2700 years ago, *Sci. Rep.*, *7*(October 2016), 1–11, doi:10.1038/srep41855.

Ekaykin, A. A., V. Y. Lipenkov, I. N. Kuzmina, S. J. Johnsen, and J. R. Petit (2004), The changes in isotope composition and accumulation of snow at Vostok station , East Antarctica , over the past 200 years, , 569–575.

Fogt, R. L., D. H. Bromwich, and K. M. Hines (2011), Understanding the SAM influence on the South Pacific ENSO teleconnection, *Clim. Dyn.*, *36*(7), 1555–1576, doi:10.1007/s00382-010-0905-0.

Fudge, T. J. et al. (2013), Onset of deglacial warming in West Antarctica driven by local orbital forcing, *Nature*, *500*(7463), 440–444, doi:10.1038/nature12376.

Garelick, H., J. Huw, D. Agnieszka, and V.-J. Eugenia (2008), Arsenic Pollution Sources, *Rev. Environ. Contam. Toxicol.*, *197*, 17–60.

Goodwin, I. A. N. D., S. Browning, A. Lorrey, and P. A. Mayewski (2012), A Reconstruction Of The Indo--Pacific Extratropical Atmospheric Longwave Pattern During The Medieval Climate Anomaly IAN D GOODWIN, STUART BROWNING,

Graf, H.-F., S. V. Shirsat, C. Oppenheimer, M. . Jarvis, R. Podzun, and D. Jacob (2010), Continental scale Antarctic deposition of sulphur and black carbon from anthropogenic and volcanic sources, , 2457–2465, doi:10.5194/acpd-9-26577-2009.

Helama, S., P. D. Jones, and K. R. Briffa (2017), Dark Ages Cold Period: A literature review and directions for future research, *Holocene*, *27*(10), 1600–1606, doi:10.1177/0959683617693898.

Hinkley, T. K., P. J. Lamothe, S. a. Wilson, D. L. Finnegan, and T. M. Gerlach (1999), Metal emissions from Kilauea, and a suggested revision of the estimated worldwide metal output by quiescent degassing of volcanoes, *Earth Planet. Sci. Lett.*, *170*(3), 315–325, doi:10.1016/S0012-821X(99)00103-X.

Hogan, A., S. Barnard, J. Samson, and W. Winters (1982), The transport of heat, water vapor and particulate material to the South Pole Plateau, *J. Geophys. Res.*, *87*(C6), 4287–4292.

Hogan, A. W. (1997), A synthesis of warm air advection to the south polar plateau, *J. Geophys. Res.*, *102*(97), 14009–14020.

Hogan, A. W., and A. J. Gow (1993), Particle transport to the snow surface at the South Pole:the beginning of a troposheric history, , 188–207.

Hong, S., T. O. Soyol-Erdene, H. J. Hwang, S. B. Hong, S. Do Hur, and H. Motoyama (2012), Evidence of global-scale as, Mo, Sb, and Tl atmospheric pollution in the antarctic snow, *Environ. Sci. Technol.*, *46*(21), 11550–11557, doi:10.1021/es303086c.

Hörz, G., and M. Kallfass (2000), The treasure of gold and silver artifacts from the Royal Tombs of Sipán, Peru - A study on the Moche metalworking techniques, *Mater. Charact.*, *45*(4–5), 391–420, doi:10.1016/S1044-5803(00)00093-0.

Hur, S. Do, X. Cunde, S. Hong, C. Barbante, P. Gabrielli, K. Lee, C. F. Boutron, and Y. Ming (2007), Seasonal patterns of heavy metal deposition to the snow on Lambert Glacier basin, East Antarctica, *Atmos. Environ.*, *41*(38), 8567–8578, doi:10.1016/j.atmosenv.2007.07.012.

Jones, P. D., and M. E. Mann (2004), Climate over past mellinia, *Rev. Geophys.*, *42*(2003), 1–42, doi:10.1029/2003RG000143.CONTENTS.

Jouzel, J. (2003), Magnitude of isotope/temperature scaling for interpretation of central Antarctic ice cores, *J. Geophys. Res.*, *108*(D12), 4361, doi:10.1029/2002JD002677.

Jouzel, J. et al. (2007), Orbital and millennial antarctic climate variability over the past 800,000 years, *Science (80-.).*, *317*(5839), 793–796, doi:10.1126/science.1141038.

Jouzel, J., G. Delaygue, A. Landais, V. Masson-Delmotte, C. Risi, and F. Vimeux (2013), Water isotopes as tools to document oceanic sources of precipitation, *Water Resour. Res.*, *49*(11), 7469–7486, doi:10.1002/2013WR013508.

Kabata-Pendias, A. (2011), *Trace elements in soils and plants*.

Koffman, B., P. Biscaye, S. Goldstein, M. Kaplan, and G. Winckler (2015), Abrupt late Holocene shift in atmospheric circulation recorded by mineral dust in the Siple Dome ice core , Antarctica, , *17*(0), 14504.

Koffman, B. G., K. J. Kreutz, D. J. Breton, E. J. Kane, D. A. Winski, S. D. Birkel, A. V. Kurbatov, and M. J. Handley (2014), Centennial-scale variability of the Southern Hemisphere westerly wind belt in the eastern Pacific over the past two millennia, *Clim. Past*, *10*(3), 1125–1144, doi:10.5194/cp-10-1125-2014.

Korotkikh, E. V., P. A. Mayewski, D. Dixon, A. V. Kurbatov, and M. J. Handley (2014), Recent increase in Ba concentrations as recorded in a South Pole ice core, *Atmos. Environ.*, *89*, 683–687, doi:10.1016/j.atmosenv.2014.03.009.

Krachler, M., J. Zheng, D. Fisher, and W. Shotyk (2009), Global atmospheric As and Bi contamination preserved in 3000 year old arctic ice, *Global Biogeochem. Cycles*, *23*(3), 1–7, doi:10.1029/2009GB003471.

Kreutz, K., P. Mayewski, I. Pittalwala, L. Meeker, M. Twickler, and S. Whitlow (2000), Sea level pressure variability in the Amundsen Sea region inferred from a West Antarctic glaciochemical record, *J. Geophys. Res.*, *105*(D3), 4047–4059, doi:10.1029/1999JD901069.

Kreutz, K. J., P. A. Mayewski, L. D. Meeker, M. S. Twickler, S. I. Whitlow, and I. I. Pittalwala (1997), Bipolar Changes in Atmospheric Circulation During the Little Ice Age, *Science (80- .).*, *277*(August), 1294–1296.

Kurbatov, A. V., P. A. Mayewski, and B. S. Abdul Jawad (2005), Ice Core Dating Software for Interactive Dating of Ice Cores, *Eos, Trans. Am. Geophys. Union. Fall Meet. Suppliment.*, *86*(52), Abstract #PP33C-1603.

Lazzara, M. A., L. M. Keller, T. Markle, and J. Gallagher (2012), Fifty-year Amundsen-Scott South Pole station surface climatology, *Atmos. Res.*, *118*, 240–259, doi:10.1016/j.atmosres.2012.06.027.

Lechleitner, F. A. et al. (2017), Tropical rainfall over the last two millennia: Evidence for a low-latitude hydrologic seesaw, *Sci. Rep.*, *7*(April), 1–9, doi:10.1038/srep45809.

Lefebvre, W., and H. Goosse (2005), Influence of the Southern Annular Mode on the sea ice-ocean system: the role of the thermal and mechanical forcing, *Ocean Sci. Discuss.*, *2*(3), 299–329, doi:10.5194/osd-2-299-2005.

Legrand, M., and S. Kirchner (1990), Legrand and Kirchner : Nitrate in South Polar Precipitation, , *95*, 3493–3507.

Legrand, M., and P. Mayewski (1997), Glaciochemistry of polar ice cores: A review, *Rev. Geophys.*, *35*(3), 219, doi:10.1029/96RG03527.

Legrand, M., C. Feniet-Saigne, E. S. Saltzman, C. Germain, N. I. Barkov, and V. N. Petrov (1991), Ice-core record of oceanic emissions of dimethylsulphide during the last climate cycle, *Nature*, *350*, 144–146.

Li, F., P. Ginoux, and V. Ramaswamy (2008), Distribution, transport, and deposition of mineral dust in the Southern Ocean and Antarctica: Contribution of major sources, *J. Geophys. Res. Atmos.*, *113*(10), 1–15, doi:10.1029/2007JD009190.

Li, F., P. Ginoux, and V. Ramaswamy (2010), Transport of Patagonian dust to Antarctica, *J. Geophys. Res. Atmos.*, *115*(18), 1–9, doi:10.1029/2009JD012356.

Lide, D. R. (2005), Abudance of elements in the Earth's crust and in the sea., in *CRC Handbook of chemistry and physics, Internet version*, Boca Raton, CRC Press.

Mann, M. E., Z. Zhang, M. K. Hughes, R. S. Bradley, S. K. Miller, S. Rutherford, and F. Ni (2008), Proxy-based reconstructions of hemispheric and global surface temperature variations over the past two millennia, *Proc. Natl. Acad. Sci.*, *105*(36), 13252–13257, doi:10.1073/pnas.0805721105.

Mann, M. E., Z. Zhang, S. Rutherford, R. S. Bradley, M. K. Hughes, D. Shindell, C. Ammann, G. Faluvegi, and F. Ni (2009), Medieval Climate Anomaly, *Science (80-.).*, *326*, 1256–1261.

Marshall, G. J. (2003a), Trends in the Soutern Annular Mode from Observations and Reanalyses, *J. Clim.*, *16*(1999), 4134–4143, doi:10.1175/1520-0442(2003)016<4134:TITSAM>2.0.CO;2.

Marshall, G. J. (2003b), Trends in the Southern Annular Mode from observations and reanalyses, *J. Clim.*, *16*(24), 4134–4143, doi:10.1175/1520-0442(2003)016<4134:TITSAM>2.0.CO;2.

Masson-Delmotte, V. et al. (2008), A review of antarctic surface snow isotopic composition: Observations, atmospheric circulation, and isotopic modeling, *J. Clim.*, *21*(13), 3359–3387, doi:10.1175/2007JCLI2139.1.

Mather, T. a. et al. (2012), Halogens and trace metal emissions from the ongoing 2008 summit eruption of Kilauea volcano, Hawaii, *Geochim. Cosmochim. Acta*, *83*, 292–323, doi:10.1016/j.gca.2011.11.029.

Matschullat, J. (2000), Arsenic in the geosphere - A review, *Sci. Total Environ.*, *249*(1–3), 297–312, doi:10.1016/S0048-9697(99)00524-0.

Matthews, J. A., and K. R. Briffa (2005), The “Little Ice Age”: Re-evaluation of an evolving concept, *Geogr. Ann. Ser. A Phys. Geogr.*, *87*(1), 17–36, doi:10.1111/j.0435-3676.2005.00242.x.

Mayewski, P. a. et al. (2004a), A 700 year record of Southern Hemisphere extratropical climate variability, *Ann. Glaciol.*, *39*(1), 127–131, doi:10.3189/172756404781814249.

Mayewski, P. a. et al. (2004b), Holocene climate variability, *Quat. Res.*, *62*(3), 243–255, doi:10.1016/j.yqres.2004.07.001.

Mayewski, P. A., and D. A. Dixon (2013), US International Trans-Antarctic Scientific Expedition (US ITASE) Glaciochemical Data, Version 2., *Boulder, Color. USA. NSIDC Natl. Snow Ice Data Center.*, doi:http://dx.doi.org/10.7265/N51V5BXR.

Mayewski, P. A., W. B. Lyons, M. J. Spencer, M. S. Twickler, C. F. Buck, and S. Whitlow (1990), An ice core record of atmospheric response to anthropogenic sulphate and nitrate, *Nature*, *346*(6284), 554–556.

Mayewski, P. A. et al. (2005), Solar forcing of the polar atmosphere, *Ann. Glaciol.*, *41*(1), 147–154, doi:10.3189/172756405781813375.

Mayewski, P. A. et al. (2013), West Antarctica’s sensitivity to natural and human-forced climate change over the Holocene, *J. Quat. Sci.*, *28*(1), 40–48, doi:10.1002/jqs.2593.

Mayewski, P. a et al. (2009), State of the Antarctic and Southern Ocean Climate System (SASOCS), *Rev. Geophys.*, *47*(2007), RG1003, doi: 10.1029/2007RG000231., doi:10.1029/2007RG000231.1.PRELUDE.

Mazzera, D. M., D. H. Lowenthal, J. C. Chow, J. G. Watson, and V. Grubĭsíc (2001), PM10 measurements at McMurdo Station, Antarctica, *Atmos. Environ.*, *35*(10), 1891–1902, doi:10.1016/S1352-2310(00)00409-X.

McWethy, D. B., C. Whitlock, J. M. Wilmshurst, M. S. McGlone, and X. Li (2009), Rapid deforestation of South Island, New Zealand, by early Polynesian fires, *The Holocene*, *19*(6), 883–897, doi:10.1177/0959683609336563.

Meyer, I., and S. Wagner (2008), The Little Ice Age in southern Patagonia: Comparison between paleoecological reconstructions and downscaled model output of a GCM simulation Three-dimensional radiocarbon modeling: A tool to assess the last glacial ocean circulation and radiocarbon chrono, *PAGES News*, *16*(2), 12–13.

Meyer, I., and S. Wagner (2009), Past Climate Variability in South America and Surrounding Regions, *Paleoenviron. Res.*, *14*, 113–128, doi:10.1007/978-90-481-2672-9.

Meyerson, E. A., P. A. Mayewski, K. J. Kreutz, L. D. Meeker, S. I. Whitlow, and M. S. Twickler (2002), The polar expression of ENSO and sea-ice variability as recorded in a South Pole ice core, *Ann. Glaciol.*, *35*, 430–436, doi:10.3189/172756402781817149.

Miller, G. H. et al. (2012), Abrupt onset of the Little Ice Age triggered by volcanism and sustained by sea-ice / ocean feedbacks, , *39*, 1–5, doi:10.1029/2011GL050168.

Miner, S. (1969), *Air pollution aspects of barium and its compounds*.

Minikin, A., M. Legrand, J. Hall, D. Wagenbach, C. Kleefeld, E. Wolff, E. C. Pasteur, and F. Ducroz (1998), Sulfur-containing species (sulfate and methanesulfonate) in coastal Antarctic aerosol and precipitation, *J. Geophys. Res. Atmos.*, *103*(D9), 10975–10990, doi:10.1029/98jd00249.

Moreno, P. I., J. P. François, R. P. Villa-Martínez, and C. M. Moy (2009), Millennial-scale variability in Southern Hemisphere westerly wind activity over the last 5000 years in SW Patagonia, *Quat. Sci. Rev.*, *28*(1–2), 25–38, doi:10.1016/j.quascirev.2008.10.009.

Morgan, V. I., I. D. Goodwin, D. M. Etheridge, and W. C.W. (1991), Evidence from Antarctic ice cores for recent increases in snow accumulation, *Nature*, *354*(6348), 569–575.

Moy, C. M., P. I. Moreno, R. B. Dunbar, M. R. Kaplan, J. Francois, R. Villalba, and T. Haberzettl (2009), *Past Climate Variability in South America and Surrounding Regions*.

Neff, P. D., and N. A. N. Bertler (2015), Trajectory modeling of modern dust transport to the Southern Ocean and Antarctica, *J. Geophys. Res.*, *120*, 9303–9322, doi:10.1002/2015JD023304.Received.

No, A., and C. Patterson (1982), Changes of lead and barium with time in California off-shore basin sediments, *Geochim. Cosmochim. Acta*, (11), 2307–2321, doi:https://doi.org/10.1016/0016-7037(82)90204-6.

Nriagu, J. O. (1989), A global assessment of natural sources of atmospheric trace metals., *Nature*, *338*, 47–49.

Nriagu, J. O., and J. M. Pacyna (1988), Quantitative assessment of worldwide contamination of air, water and soils by trace elements., *Nature*, *333*, 134–139.

Olmez, I., D. L. Finnegan, and W. H. Zoller (1986), Iridium emissions from Kilauea volcano, *J. Geophys. Res.*, *91*(B1), 653–663.

Ommen, T., and V. I. Morgan (1997), Seasonality in late-Ho;ocene climate from ice-core records, *The Holocene*, *7*(3), 351–354.

Osterberg, E. C., M. J. Handley, S. B. Sneed, P. A. Mayewski, and K. J. Kreutz (2006), Continuous ice core melter system with discrete sampling for major ion, trace element, and stable isotope analyses, *Environ. Sci. Technol.*, *40*(10), 3355–3361, doi:10.1021/es052536w.

Pacyna, J. M. (1987), Atmospheric Emissions of Arsenic , Generation and Industry, , 69–88.

Pacyna, J. M., and E. G. Pacyna (2001), An assessment of global and regional emissions of trace metals to the atmosphere from anthropogenic sources worldwide, *Environ. Rev.*, *9*(4), 269–298, doi:10.1139/er-9-4-269.

Petit, R. J. et al. (1999), Climate and atmospheric history of the past 420,000 years from the Vostok ice core, Antarctica, *Nature*, *399*(6735), 429–413, doi:10.1038/20859.

Pfahl, S., and H. Sodemann (2014), What controls deuterium excess in global precipitation?, *Clim. Past*, *10*(2), 771–781, doi:10.5194/cp-10-771-2014.

Planchon, F. A. M., C. F. Boutron, C. P. Ferrari, C. Barbante, G. Cozzi, P. Cescon, and E. W. Wolff (2002a), Changes in heavy metals in Antarctic snow from Coats Land since the mid-19th to the late-20th century, *Earth Planet. Sci. Lett.*, *200*(1–2), 207–222, doi:10.1016/S0012-821X(02)00612-X.

Planchon, F. a M., C. F. Boutron, C. Barbante, G. Cozzi, V. Gaspari, E. W. Wolff, C. P. Ferrari, and P. Cescon (2002b), Changes in heavy metals in Antarctic snow from Coats Land since the mid-19th to the late-20th century, *Earth Planet. Sci. Lett.*, *200*(1–2), 207–222, doi:10.1016/S0012-821X(02)00612-X.

Potocki, M., P. A. Mayewski, A. V. Kurbatov, J. C. Simões, D. A. Dixon, I. Goodwin, A. M. Carleton, M. J. Handley, R. Jaña, and E. V. Korotkikh (2016), Recent increase in Antarctic Peninsula ice core uranium concentrations, *Atmos. Environ.*, *140*, 381–385, doi:10.1016/j.atmosenv.2016.06.010.

Prospero, J. M., P. Ginoux, O. Torres, S. E. Nicholson, and T. E. Gill (2002), Environmental characterization of global sources of atmospheric soil dust identified with the Nimbus 7 Total Ozone Mapping Spectrometer (TOMS) absorbing aerosol product, *Rev. Geophys.*, *40*(1), 1–31, doi:10.1029/2000RG000095.

Raphael, M. N., G. J. Marshall, J. Turner, R. L. Fogt, D. Schneider, D. A. Dixon, J. S. Hosking, J. M. Jones, and W. R. Hobbs (2016), The Amundsen sea low: Variability, change, and impact on Antarctic climate, *Bull. Am. Meteorol. Soc.*, *97*(1), 111–121, doi:10.1175/BAMS-D-14-00018.1.

Reimann, C., J. Matschullat, M. Birke, and R. Salminen (2009), Arsenic distribution in the environment: The effects of scale, *Appl. Geochemistry*, *24*(7), 1147–1167, doi:10.1016/j.apgeochem.2009.03.013.

Reimer, P. J. et al. (2004), IntCal04 terrestrial radiocarbon age calibration, 0-26 cal kyr BP, *Radiocarbon*, doi:10.1017/S0033822200032999.

RICE community members (2018), The Ross Dipole - temperature, snow accumulation, and sea ice variability in the Ross Sea Region, Antarctica, over the past 2700 years, *Clim. Past*, *14*, 193–214, doi:10.5194/cp-14-193-2018.

Rong, H., H. Shugui, L. Yuansheng, P. Hongxi, P. Mayewski, S. Sneed, A. Chunlei, and M. Handley (2016), Arsenic record from a 3 m snow pit at Dome Argus, Antarctica, *Antarct. Sci.*, 1–8, doi:10.1017/S0954102016000092.

Schroeder, H. A. (1970), *No Barium. Air quality monograph.*, Air Qualit., American Petrolium Institute, Washington, DC.

Schwanck, F., J. C. Simões, M. Handley, P. A. Mayewski, R. T. Bernardo, and F. E. Aquino (2016), Anomalously high arsenic concentration in a West Antarctic ice core and its relationship to copper mining in Chile, *Atmos. Environ.*, *125*, 257–264, doi:10.1016/j.atmosenv.2015.11.027.

Shaw, G. E. (1988), Antarctic aerosols: A review, *Rev. Geophys.*, *26*(1), 89–112.

Shulmeister, J. (1999), Australasian evidence for mid-Holocene climate change implies precessional control of Walker Circulation in the Pacific, *Quat. Int.*, *57–58*, 81–91, doi:10.1016/S1040-6182(98)00052-4.

Shulmeister, J. et al. (2004), The Southern Hemisphere westerlies in the Australasian sector over the last glacial cycle: A synthesis, *Quat. Int.*, *118–119*, 23–53, doi:10.1016/S1040-6182(03)00129-0.

Siggaard-Andersen, M. L., P. Gabrielli, J. P. Steffensen, T. Strømfeldt, C. Barbante, C. Boutron, H. Fischer, and H. Miller (2007), Soluble and insoluble lithium dust in the EPICA DomeC ice core-Implications for changes of the East Antarctic dust provenance during the recent glacial-interglacial transition, *Earth Planet. Sci. Lett.*, *258*(1–2), 32–43, doi:10.1016/j.epsl.2007.03.013.

Sigl, M. et al. (2013), A new bipolar ice core record of volcanism from WAIS Divide and NEEM and implications for climate forcing of the last 2000 years, *J. Geophys. Res. Atmos.*, *118*(3), 1151–1169, doi:10.1029/2012JD018603.

Sime, L. C., K. E. Kohfeld, C. Le Quéré, E. W. Wolff, A. M. de Boer, R. M. Graham, and L. Bopp (2013), Southern Hemisphere westerly wind changes during the Last Glacial Maximum: Model-data comparison, *Quat. Sci. Rev.*, *64*, 104–120, doi:10.1016/j.quascirev.2012.12.008.

Sodemann, H., and A. Stohl (2009), Asymmetries in the moisture origin of Antarctic precipitation, , *36*(October), 1–5, doi:10.1029/2009GL040242.

Steig, E. J., D. L. Morse, E. D. Waddington, M. Stuiver, P. M. Grootes, P. A. Mayewski, M. S. Twickler, and S. I. Whitlow (2000), Wisconsinan and Holocene Climate History from an Ice Core at Taylor Dome, Western Ross Embayment, Antarctica, *Geogr. Ann. Ser. A Phys. Geogr.*, *82*(2–3), 213–235, doi:10.1111/j.0435-3676.2000.00122.x.

Stenni, B. et al. (2011), Expression of the bipolar see-saw in Antarctic climate records during the last deglaciation, *Nat. Geosci.*, *3*(12), 1–4, doi:10.1038/ngeo1026.

Sudarchikova, N., U. Mikolajewicz, C. Timmreck, D. O'Donnell, G. Schurgers, D. Sein, and K. Zhang (2015), Modelling of mineral dust for interglacial and glacial climate conditions with a focus on Antarctica, *Clim. Past*, *11*(5), 765–779, doi:10.5194/cp-11-765-2015.

Swart, N. C., J. C. Fyfe, N. Gillett, and G. J. Marshall (2015), Comparing trends in the southern annular mode and surface westerly jet, *J. Clim.*, *28*(22), 8840–8859, doi:10.1175/JCLI-D-15-0334.1.

Thompson, D. W. J., and J. M. Wallace (2000), Annular modes in the extratropical circulation. Part II: Trends, *J. Clim.*, *13*(5), 1018–1036, doi:10.1175/1520-0442(2000)013<1018:AMITEC>2.0.CO;2.

Trouet, V., J. Esper, N. E. Graham, A. Baker, J. D. Scourse, and D. C. Frank (2009), Persistent positive north atlantic oscillation mode dominated the medieval climate anomaly, *Science (80-.).*, *324*(5923), 78–80, doi:10.1126/science.1166349.

Tuncel, G., N. K. Aras, and W. H. Zoller (1989), Temporal variations and sources of elements in the South Pole atmosphere: 1. Nonenriched and moderately enriched elements, *J. Geophys. Res. Atmos.*, *94*(D10), 13025–13038, doi:Doi 10.1029/Jd094id10p13025.

Turner, J., T. Phillips, J. S. Hosking, G. J. Marshall, and A. Orr (2013), The amundsen sea low, *Int. J. Climatol.*, *33*(7), 1818–1829, doi:10.1002/joc.3558.

Vallelonga, P., K. Van de Velde, J. P. Candelone, V. I. Morgan, C. F. Boutron, and K. J. R. Rosman (2002), The lead pollution history of Law Dome, Antarctica, from isotopic measurements on ice cores: 1500 AD to 1989 AD, *Earth Planet. Sci. Lett.*, *204*(1–2), 291–306, doi:10.1016/S0012-821X(02)00983-4.

Varma, V., M. Prange, T. Spangehl, F. Lamy, U. Cubasch, and M. Schulz (2012), Impact of solar-induced stratospheric ozone decline on Southern Hemisphere westerlies during the Late Maunder Minimum, , *39*(October), 1–6, doi:10.1029/2012GL053403.

Van de Velde, K., P. Vallelonga, J. P. Candelone, K. J. R. Rosman, V. Gaspari, G. Cozzi, C. Barbante, R. Udisti, P. Cescon, and C. F. Boutron (2005), Pb isotope record over one century in snow from Victoria Land, Antarctica, *Earth Planet. Sci. Lett.*, *232*(1–2), 95–108, doi:10.1016/j.epsl.2005.01.007.

Vimeux, F., V. Masson, G. Delaygue, J. Jouzel, J. R. Petit, and M. Stievenard (2001), A 420,000 year deuterium excess record from East Antarctica: Information on past changes in the origin of precipitation at Vostok, *J. Geophys. Res.*, *106*(D23), 31863, doi:10.1029/2001JD900076.

Wai, K. M., S. Wu, X. Li, D. A. Jaffe, and K. D. Perry (2016), Global Atmospheric Transport and Source-Receptor Relationships for Arsenic, *Environ. Sci. Technol.*, *50*(7), 3714–3720, doi:10.1021/acs.est.5b05549.

Wanner, H., O. Solomina, M. Grosjean, S. P. Ritz, and M. Jetel (2011), Structure and origin of Holocene cold events, *Quat. Sci. Rev.*, *30*(21–22), 3109–3123, doi:10.1016/j.quascirev.2011.07.010.

Wardell, L. J., P. R. Kyle, and D. Counce (2008), Volcanic emissions of metals and halogens from White Island (New Zealand) and Erebus volcano (Antarctica) determined with chemical traps, *J. Volcanol. Geotherm. Res.*, *177*(3), 734–742, doi:10.1016/j.jvolgeores.2007.07.007.

Wedepohl, K. H. (1995), The composition of the continental crust, *Geochim. Cosmochim. Acta*, *59*(7), 1217–1232.

Welch, K. A., P. A. Mayewski, and S. I. Whitlow (1993), Methanesulfonic acid in coastal antarctic snow related to sea-ice extent., *Geophys. Res. Lett.*, *20*(6), 443–446.

Wessel, P., W. H. F. Smith, R. Scharroo, J. Luis, and F. Wobbe (2013), Generic Mapping Tools: Inproved version released, *EOS Trans. AGU*, *94*(45), 409–410, doi:10.1002/2013EO450001.

Wolff, E. W., and H. Cachier (1998), Concentrations and seasonal cycle of black carbon in aerosol at a coastal Antarctic station, *J. Geophys. Res.*, *103*(D9), 11033, doi:10.1029/97JD01363.

Wolff, E. W., E. D. Suttie, and D. a. Peel (1999), Antartic snow record of cadmium, copper and zinc content during the twentieth century, *Atmos. Environ.*, *33*, 1535–1541.

Wolff, E. W. et al. (2006), Southern Ocean sea-ice extent, productivity and iron flux over the past eight glacial cycles., *Nature*, *440*(7083), 491–496, doi:10.1038/nature06271.

Yan, H., L. Sun, Y. Wang, W. Huang, S. Qiu, and C. Yang (2011), A record of the Southern Oscillation Index for the past 2,000 years from precipitation proxies, *Nat. Geosci.*, *4*(9), 611–614, doi:10.1038/ngeo1231.

Zhang, S. Y., G. X. Sun, X. X. Yin, C. Rensing, and Y. G. Zhu (2013), Biomethylation and volatilization of arsenic by the marine microalgae Ostreococcus tauri, *Chemosphere*, *93*(1), 47–53, doi:10.1016/j.chemosphere.2013.04.063.

Zreda-Gostynska, G., P. R. Kyle, D. Finnegan, and K. M. Prestbo (1997), Volcanic gas emissions from Mount Erebus and their impact on the Antarctic environment, *J. Geophys. Res.*, *102*(B7), 15039, doi:10.1029/97JB00155.

BIOGRAPHY OF THE AUTHOR

Elena Korotkikh was born in Kemerovo, Russia on September 29, 1979. She graduated from Novosibirsk State University with the Bachelor degree in geology and geochemistry of oil and gas in 2004. She received a Master of Science degree in Quaternary and Climate Studies from the University of Maine in August, 2009. Elena Korotkikh is a candidate for the Doctor of Philosophy degree in Earth and Climate Sciences from The University of Maine in August 2019.